VOLUME 21, 1959/60, No. 9 pp. 253-280 Published 4th August 1960

Philips Technical Review

DEALING WITH TECHNICAL PROBLEMS
RELATING TO THE PRODUCTS, PROCESSES AND INVESTIGATIONS OF
THE PHILIPS INDUSTRIES

AN AUTOMATIC PARTICLE COUNTER AND SIZER

by H. A. DELL *), D. S. HOBBS *) and M. S. RICHARDS *).

531.717:531.791:621.317.39

Considerable attention has been paid in the last decade or so to the problem of automatically performing counting and sizing of samples of particles. This article gives an introduction to the problem and describes an advanced instrument for this purpose developed by the Mullard Research Laboratories.

In many investigations it is useful to be able to count and find the size distribution of numbers of particles [1]). The counting of blood cells, the measurement of the pigment granules in paints and the assessment of the explosion and health hazards of dust-laden coal-mine air are typical instances.

At some stage of each of these investigations a prepared sample from the medium in question is laid out on a flat surface. This two-dimensional specimen is then examined point by point by some microscopic or similar means. From the method of preparation and the features discovered in a known area of the two-dimensional specimen, the character of the original sample is determined.

It can be seen that the act of examining a plane field of view point by point is in many ways analogous to that of scanning a scene or picture as is done in television or phototelegraphic techniques. It is not surprising, therefore, that many methods based on these techniques should have been suggested for *automatically* analysing two-dimensional specimens of this type.

After a discussion of the nature of the problem, some of the methods used for the automatic counting and sizing of particles will be outlined. The methods used in the Mullard equipment will then be described more fully and further details given of the construction of this equipment. *Fig. 1* shows a photograph of the Mullard particle analyser.

Statement of the problem

For both the counting and the sizing of particles some type of scanning procedure is required. Furthermore it is necessary to have some method of ensuring that a particle is not counted more than once, or that two or more particles are not lumped together as one. When counting visually through a microscope, the observer's eyes perform the scanning function, while his memory of the counted particles in the whole field has to preclude duplicate or lumped counts. This can be very fatiguing and is not always very reliable, especially when the sample consists of a large number of particles (as is desirable to keep statistical errors low).

In an automatic apparatus for counting and sizing the scanning may be performed by a light beam, the modulation of which by the particles is detected by some type of photocell. Two systems that have been described are the line scan and the spot scan. In the former, a long narrow illuminated aperture is moved at right angles to its length, sweeping out an area as it does so. In the other, a small spot of light is moved over the specimen in a series of parallel lines until the required field has been covered. With the line scanning system duplication of counts gives less trouble than the counting of two or more particles as one, but certain artifices may be employed to

*) Mullard Research Laboratories, Salfords, Surrey, England.

1) For a comprehensive review of the whole subject of particle size analysis, see The physics of particle size analysis, Brit. J. appl. Phys., Suppl. No. 3, 1954. See also G. Herdan, Small particle statistics, Elsevier, Amsterdam 1953. A recent review of automatic sizing methods is given by B. B. Morgan, Research (London) **10**, 271-279, 1957.

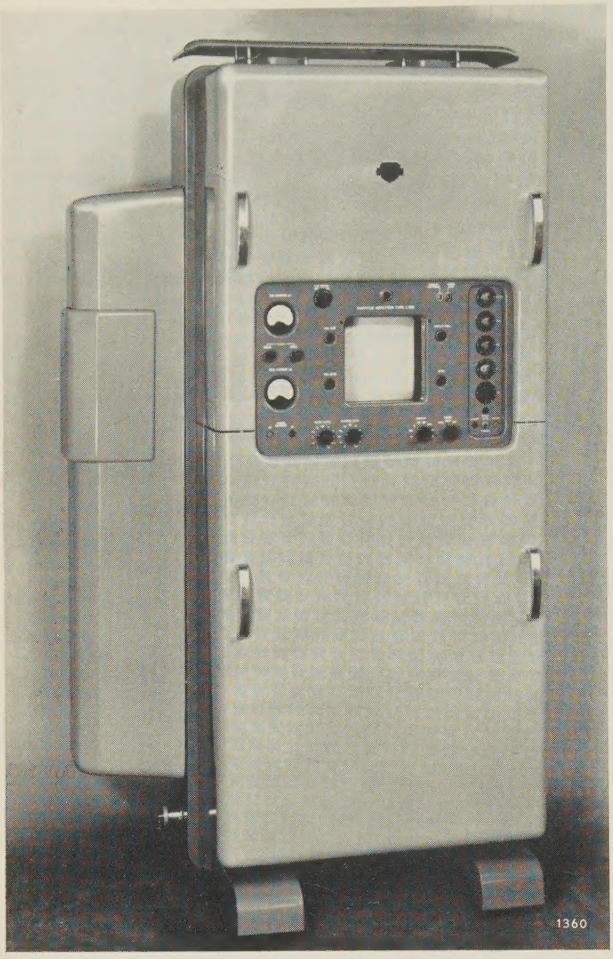

Fig. 1. Photograph of the Mullard particle analyser, type L 188.

reduce such errors. In the spot scanning system, duplicate, multiple or lumped counts can be largely eliminated with the aid of a line-to-line "memory".

For automatic *sizing* of particles each particle encountered has to be "explored" in some way and quantitatively assessed. In the Mullard instrument this is done by measuring the length of the intercepts of each particle. Another method is that whereby the scanning spot is momentarily deflected perpendicular to the scan direction as it encounters a particle and hence measures a "diameter" of the particle. Several other systems are possible. In all these methods, however, an important simplification is achieved by successive scanning of the whole field, each time for particles greater than a certain pre-set size. Each complete scan thus counts all particles greater than the pre-set size; from the successive scans an integrated size distribution curve can be plotted.

The accuracy of counting and sizing depends on the resolution of the instrument in relation to the particle size, the size of the field in relation to the particle size (edge effects) and the number of particles in the field (sampling errors and edge effects). Clearly these various errors can be diminished by examining different parts of the sample and by multiple sampling.

Scanning of the sample

The line scanning method is illustrated diagrammatically in *fig. 2*. An idealized specimen containing three particles A, B and C is shown at (a), while (b) indicates the light signals that would be generated by such a specimen as it was scanned.

It can be seen that while particle A generates a unique signal from which its dimensions could be determined, particles B and C generate a combined signal, from which their individual dimensions, or even their separate presence, cannot be deduced directly. If all individual particles are of interest, it is necessary then to make sure that only one is intercepted by the illuminated aperture at once, or to include some statistical correction for multiple interceptions.

In the same way, particles only partially intercepted at the ends of the line cause inaccurate signals, as they are indistinguishable from smaller particles fully intercepted.

Two methods have been suggested for dealing with this latter effect. One is to perform two (or more) experiments using different lengths of swept line [2]). If it can be assumed that the end effects are statistically the same in both instances, then the difference between the results will give the effect of sweeping the specimen with a line of length equal to the difference between the two lengths actually used but possessing no end effects. When such a system is used it is important that the larger line should not substantially alter the chances of intercepting more than one particle at a time, as may easily occur with non-uniform specimens.

The other method suggested and also used in a commercial instrument [3]) uses a triple swept line system. In this, the main measuring line has associated with it two short guard lines, one at either end. They and the measuring line form a single exploring system which is swept across the specimen. The circuit logic ensures that particles intercepted by the main line and one, or both, of the guard lines are disregarded. Thus only particles intercepting the main line alone are recorded by the apparatus. This technique suffers from the disadvantage that the exact area of the specimen effectively scanned is larger for small particles than for large ones, so that once again a measure of uncertainty is introduced.

In view of these shortcomings the Mullard particle analyser uses the spot scanning method (*fig. 3*).

[2]) H. S. Wolff, Nature **165**, 967, 1950. A commercial instrument using this system is described by P. G. W. Hawksley *et al.*, Brit. J. appl. Phys., Suppl. No. 3, p. S.165, 1954, and B. B. Morgan and E. W. Meyer, J. sci. Instr. **36**, 492, 1959. The theory of the method was given by P. G. W. Hawksley, Brit. J. appl. Phys., Suppl. No. 3, p. S.125, 1954.

[3]) E. W. Meyer, British Patent 714 350, 1951. Edge effects are also discussed by H. Nassenheim, Chem. Ing. Tech. **27**, 38-39, 535-542, 787-794, 1955.

A specimen containing four particles *A*, *B*, *C* and *D* is shown at (*a*), while (*b*) indicates the signals that are generated when the specimen is scanned by a very small spot.

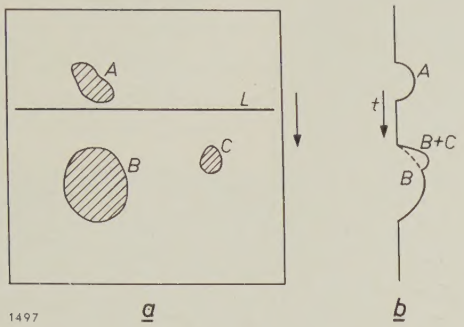

Fig. 2. Illustrating the *line* scanning method. *a*) Idealized particle sample. *L* is a line of light moving in the direction of the arrows. *b*) Signals obtained as the scanning proceeds.

In this case the source of any signal can always be identified uniquely with a definite location in the image plane, determined by the spot position. Within certain limits of resolution determined by the finite spot size and scan line spacing, neighbouring particles can always be separately distinguished. In fact, within these limits, the signals generated must contain all information about the particles present, for a specimen image can be reconstructed from them (cf. facsimile telegraphy and television). Unfortunately, information about particle numbers and sizes can be extracted only with some difficulty.

The reason for this is that large particles overlap several lines of scan and so produce signals on each interception. If the size of each particle were required, it would be necessary in addition to store up all the intercept information due to any one particle. On completing the scan either the number or the magnitude of the intercepts on each particle could then be determined. (As will be seen presently, the present instrument sizes by intercept "maximization"; this does not require storage of *all* the intercept information from each particle but only line-to-line storage.)

If the nature of the specimen is well established beforehand (in particular if the shape of the particles is more or less invariant, e.g. circular), this recognition of multiple interception can be based purely on a statistical analysis related to intercept length [4]). It is then only necessary to count and measure all the interceptions found in a field of view to be able to infer the number and size distribution of the particles present. More often, as the very nature of the specimen is the point in question, this is impossible. A more precise recognition of signal association then becomes necessary.

Line-to-line signal association

In order to count and size in an automatic machine, it is necessary to lay down some *criterion* by which successive interceptions may be judged as belonging to the same or different particles.

Two different criteria have been considered in the literature. The first, called the "anticipation-tolerance" criterion [5]), states that a signal in any line of scan must be regarded as due to a large particle overlapping the previous line of scan only if a signal occurred in the previous line whose leading edge (say), as measured along the line, lay within a predetermined tolerance distance from the leading edge of the later signal.

In the instance illustrated (fig. 3), a tolerance may be selected which would, for example, correctly associate the first signal in line *8* with that in line 7, but which would rightly exclude the second signal in line *8*, recognizing it as due to a separate particle. If particles exist having extended edges nearly parallel to the lines of scan, a large tolerance is necessary. It may then be very difficult to avoid incorrectly associating signals due to separate but nearby particles. Similar difficulties arise if trailing-edge signals are used.

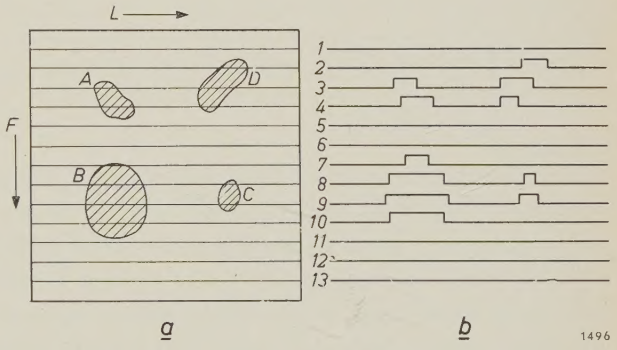

Fig. 3. Illustrating the *spot* scanning method. *a*) Idealized sample. *L* is the line scan direction and *F* the frame scan direction. *b*) Signals obtained from the particles shown.

The second, the "overlap" criterion (the advantages of which were first emphasized by Roberts [6])), states that a signal in any line of scan must be regarded as due to a large particle overlapping the previous line of scan only if a signal occurred in the previous line *some part of which* lay the same distance

[4]) J. G. Dawes and P. G. W. Hawksley, reported in W. H. Walton, Central Research Establishment Report of National Coal Board (U.K.) No. 79, 12 June 1951.

[5]) D. W. Gillings, British Patent 719 773, 1950.

[6]) F. Roberts, reported in W. H. Walton, Nature **169**, 518, 1952.

along the line as *some part* of the later signal (i.e. some signal overlap existed). When a light spot of finite size is used to scan lines spaced by approximately the spot *radius*, it can be shown that the overlap criterion will correctly interpret all signals down to a resolving limit of about the spot *diameter*. The false association possibility inherent in the anticipation-tolerance criterion, which may become very significant when dense specimens are considered, is small in this case.

The overlap criterion is the superiorw hen counting only is required, but when *sizing* by intercept *summation* it runs into difficulties. For this reason, all the intercept-summing sizing systems so far described in the literature use the anticipation-tolerance criterion [5] [7] [8].

Consider, for example, the signals due to the particle *D* in fig. 3. In the second line of scan of the field the first intercept signal from this particle occurs and must be suitably stored away. In the third line of scan, the second intercept signal will occur, but only after a certain delay (here just over half the duration of this signal) will association with the first intercept be recognized. Until that moment it could have been due to a new and different particle. All of the signal must be stored correctly, however, for otherwise a later signal, such as that in the fourth line, may never be recognized as due to part of the same particle. Some temporary store is thus necessary in which all signals can be held until their ultimate destination is known.

This difficulty does not arise with the anticipation-tolerance criterion. A signal in any line of scan either lies within the tolerance zone of a previous interception, when the correct destination is known, or it lies outside all such zones, when it must represent a new particle. In either case the appropriate action is established from the *beginning* of the signal.

The present instrument, however, sizes by intercept "maximization", that is, each intercept pulse is compared in length to a certain pre-set value and a count is made only when this pre-set value is exceeded [9]. As a result it is only necessary to store intercept information for the duration of *one* line of scan, and there is then no fundamental difficulty in applying the overlap criterion.

Spot scanning systems in general suffer from the disadvantage that an indented particle may be met in such a fashion that it initially appears to the scanner as two or more separate particles (see *fig. 4*). Only when the full bulk is discovered may their unity be recognized. This difficulty is not easily overcome, although the errors it causes are not so serious because such indented "particles" are often, in fact, agglomerates.

Line-to-line memory

Whichever criterion of signal association is used, some form of memory is necessary in which it is possible to store the signals generated by the scanning system. During the scanning of any line this record must then be read, so that a representation of the signal generated one line previously is available.

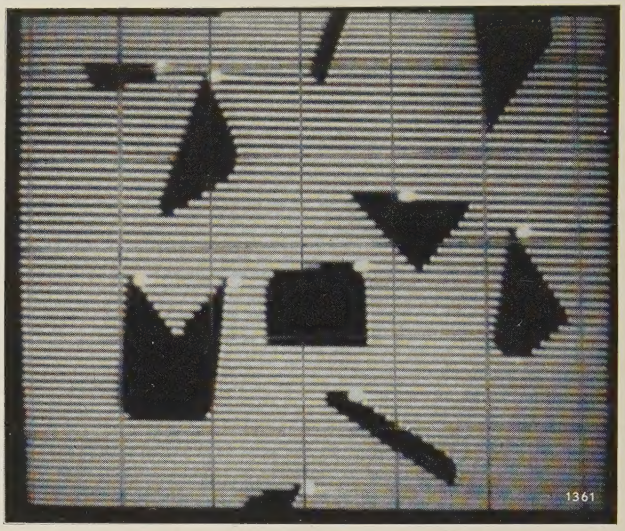

Fig. 4. Scanning of idealized particles, displayed on a monitor tube. Direction of scanning; right to left. The white dots are marker tags to indicate when a count has been made (see below). It will be noted that the indented particle (lower left) has been counted twice.

In a particle analyser these remembered signals are compared with the output of the scanner. For every particle, only on the first intercept does a scanner signal exist which has no counterpart in the memory. This condition may be made to generate a unique impulse corresponding to each particle. (During scanning of the line following the last intercept there also occurs a signal unique to each particle; in this case it is the delayed signal from the previous line, the direct signal being zero.)

In addition to true line-to-line memory systems a double-spot pseudo-memory [10] may be used. In this the specimen is scanned by two similar but identifiable light spots and the light signals transmitted at the two scanning points are indicated in two separate channels. If as one spot scans the n-th line of the raster and the other (trailing) spot similarly scans the $(n-1)$th line, signals are available in the two channels which correspond to those which a single-spot scanner and a memory would produce.

This simple method of imitating the action of a memory suffers from a practical disadvantage, first pointed out by

[7]) C. F. Bareford and H. A. Dell, British Patent 727 134, 1951.
[8]) W. H. Walton, D. G. A. Thomas and J. W. Philips, British Patent 732 662, 1951.
[9]) D. S. Hobbs, British Patent Appl. 16101/56.
[10]) H. A. Dell and E. Jones, British Patent 741 471, 1951.

Walton (private communication), which is more serious than would appear. The signal delivered by the trailing spot is not the remembered signal which the leading spot delivered; it is instead a "repetition" of that signal produced by the trailing spot. If, therefore, the trailing spot either takes a slightly different path from the leading spot, or possesses a slightly different signal sensitivity (both conditions almost impossible to avoid in practice), the reconstructed signal may be false. The result of this potential fallibility is that in many instances particles may be counted twice or missed altogether.

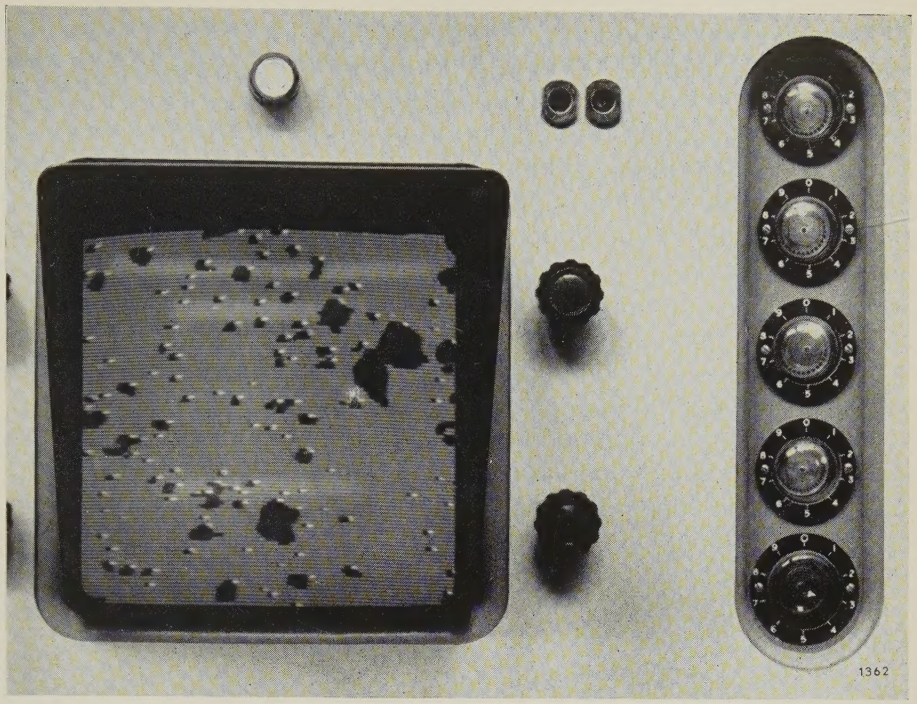

Fig. 6. Display panel showing the 12″ monitor tube and the dekatron counters. As each particle is counted it is "tagged" with a bright spot by a strobe pulse from the counter. The photograph was taken with an exposure time corresponding to more than 20 frames. The sharpness of outline indicates the stability of the instrument.

Many different forms of line-to-line signal memories have been tried. These include magnetic drum and tape recorders, electrostatic cathode-ray tube storage systems [11]), acoustic delay lines of the wire type [12]) and mercury delay lines. Of all these, mercury acoustic delay lines have proved the most satisfactory for this application. Such a delay line, providing a delay of 1000 μsec, is employed in the Mullard instrument for the line-to-line memory and will be described later in this article.

The Mullard particle analyser

In the Mullard instrument a photograph of the sample is first made on standard 35 mm film and it is this photograph that is examined by the instrument. The philosophy behind this is that it leaves the user greater freedom in sampling methods and in exploiting the various techniques available to the microscopist. This makes the instrument more versatile, for it would be impracticable to build in elaborate optical facilities into what is already quite a complicated instrument, quite apart from the costs involved and the undesirable duplication of equipment already available in most laboratories.

The film is scanned by a flying-spot scanner [13]). A scanning raster of 100 lines, 60 × 60 mm is produced on the face of a cathode-ray tube, type MC 13-16, which has a very short-persistence phosphor [14]). The frame frequency is nearly 10 c/s, so that the whole field is scanned in about 1/10 sec. The raster is projected in reduced format by an optical system (*fig. 5*) onto the 20 × 20 mm image on the film. The transmitted light falls on a photomultiplier tube producing a signal related to the local opacity of the area scanned at any moment.

For monitoring purposes, a 12″ cathode-ray tube displays the scanned area at a linear magnification of 10× (*fig. 6*). Each particle is "tagged" with a bright marker spot as it is counted. When

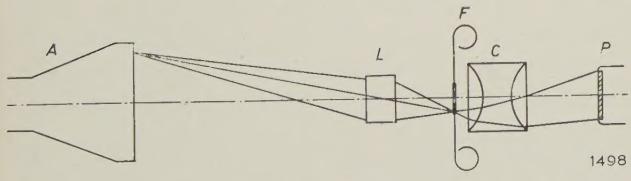

Fig. 5. Flying-spot scanner showing the optical system which reduces the 60 × 60 mm raster on the cathode-ray tube to a 20×20 mm image on the film. *A* scanner tube. *L* projection lens. *F* film sample. *C* condenser. *P* photomultiplier. In the actual instrument two projection lenses are provided in a turret mount, the second lens giving a reduction of about 12×. The raster image on the film is then only 5 × 5 mm, so that the resolution is higher.

[11]) F. C. Williams and T. Kilburn, Proc. Instn. Electr. Engrs. **96**-III, 81, 1949.

[12]) E. M. Bradburd, Electrical Communication **28**, 46, 1951.

[13]) The principles of this type of scanner are outlined in F. H. J. van der Poel and J. J. P. Valeton, Philips tech. Rev. **15**, 221, 1953/54.

[14]) A. Bril, J. de Gier and H. A. Klasens, Philips tech. Rev. **15**, 233, 1953/54.

sizing, the bright tags appear only on those particles with intercepts greater than the pre-selected value. With the normal projection lens (20×20 mm raster on film), the size pre-set control gives a series of eleven critical sizes, increasing by a factor $\sqrt{2}$, viz. 0.2 mm, 0.28, 0.40, 0.56, 0.80, 1.14, 1.60, 2.28, 3.20, 4.56, 6.40 mm.

The results of counting or sizing appear on decade counters situated on the display panel (fig. 6). The count appearing there is in fact the totalled count obtained by scanning the field ten times, the repetitive scanning being performed automatically. The reading therefore has to be divided by ten. The reading is displayed for seven seconds, after which the cycle of ten scans repeats automatically. Alternatively, the reading can remain in the counters until reset manually after changing the sample or changing the pre-set size.

With the aid of the simplified block diagram in *fig. 7*, we shall now describe the operation of the particle analyser, leaving certain circuits and components to be described later when their functions and critical requirements will be more evident.

In order to understand how the instrument works, we must first consider in detail the system used for line-to-line signal association. It will then be clear how the instrument makes a simple *count* of the particles of a sample. To understand how the instrument measures a *size distribution*, we must further consider details of the sizing discriminator and certain associated circuitry which ensure that counts are registered only for particles greater than a certain pre-set size.

To simplify the explanations, we consider the pulses from only a few representative particles over a small portion of the scan.

Counting

Referring to the block diagram of fig. 7, we imagine the two-pole switch S to be in the right-hand position ("Count"). Of the four channels carrying the shaped intercept signals, only *1* and *2* are now

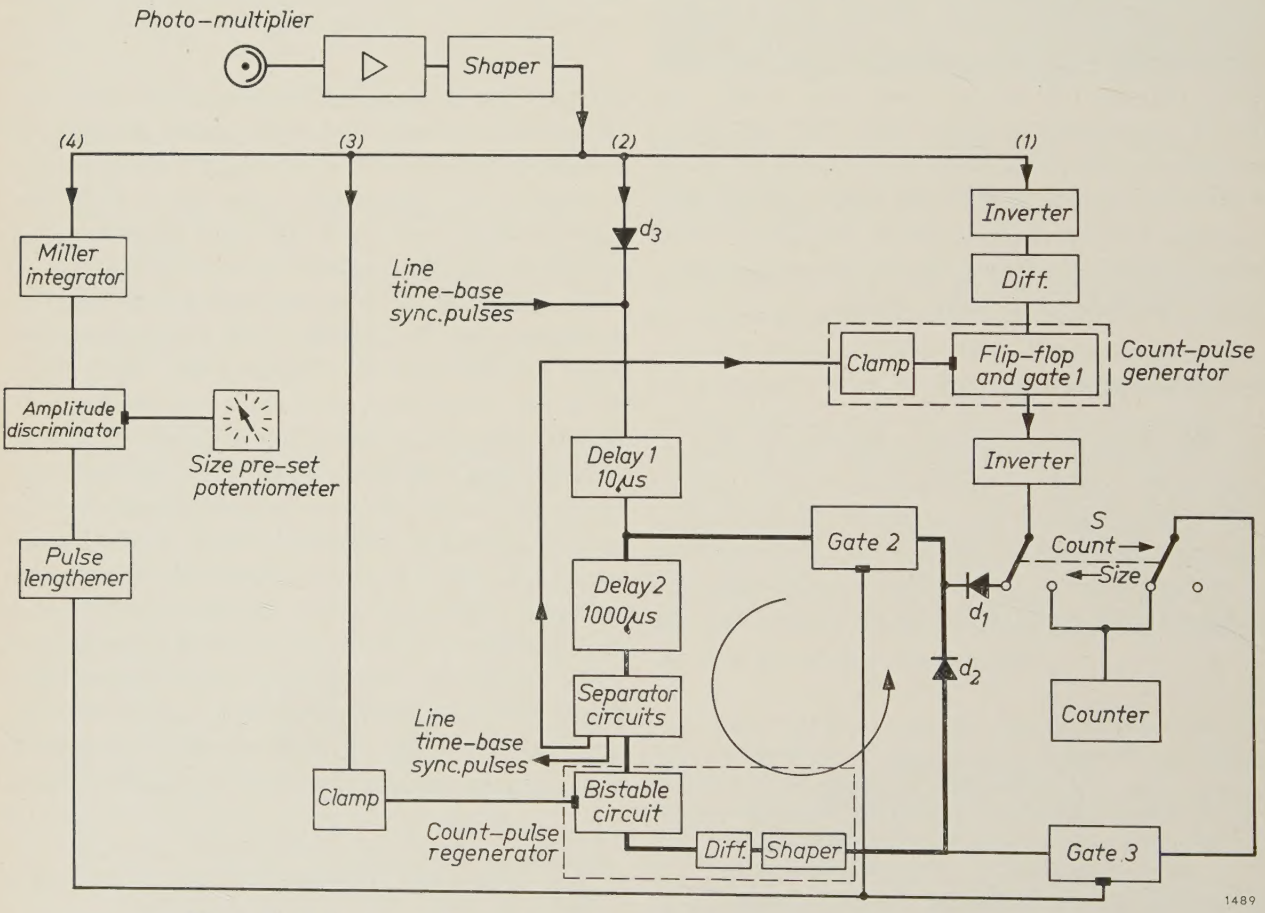

Fig. 7. Block diagram of the particle analyser. The particle-intercept signals produced in the photomultiplier of the flying-spot scanner are amplified, and then shaped by clipping. The shaped pulses are then fed to four channels: (*1*) the count-pulse channel, (*2*) the delay-line channel, (*3*) the recirculation-clamp channel and (*4*) the size-discriminator channel. During *counting* (switch S to right), only channels *1* and *2* are performing any function. In *sizing* (S as drawn) all four channels are functioning. Delay *1* is a lumped-parameter delay line; delay *2* is a mercury delay line.

operative. In channel *1* each intercept signal is inverted and differentiated. The resulting pulses are fed to gate *1* (which is always closed to negative pulses). The positive (trailing edge) pulse forms the "count pulse" and is allowed to pass gate *1* to the counter only if this gate has been opened [15]) by the leading-edge pulse operating an Eccles-Jordan flip-flop (see *fig. 8a*); the latter, however, can be operated only provided that it has not been clamped by an in fact cuts off its tail so as to give the count pulse a duration of about 3 μsec. On the second and succeeding intercepts of a particle (fig. 8*c*) the flip-flop is clamped by the presence of a delayed intercept pulse carried over from the previous line of scan, some part of which overlaps some part of the direct intercept pulse: *either* the delayed signal overlaps the leading edge of the direct signal *or* the direct signal overlaps the leading edge of the delayed signal [16]).

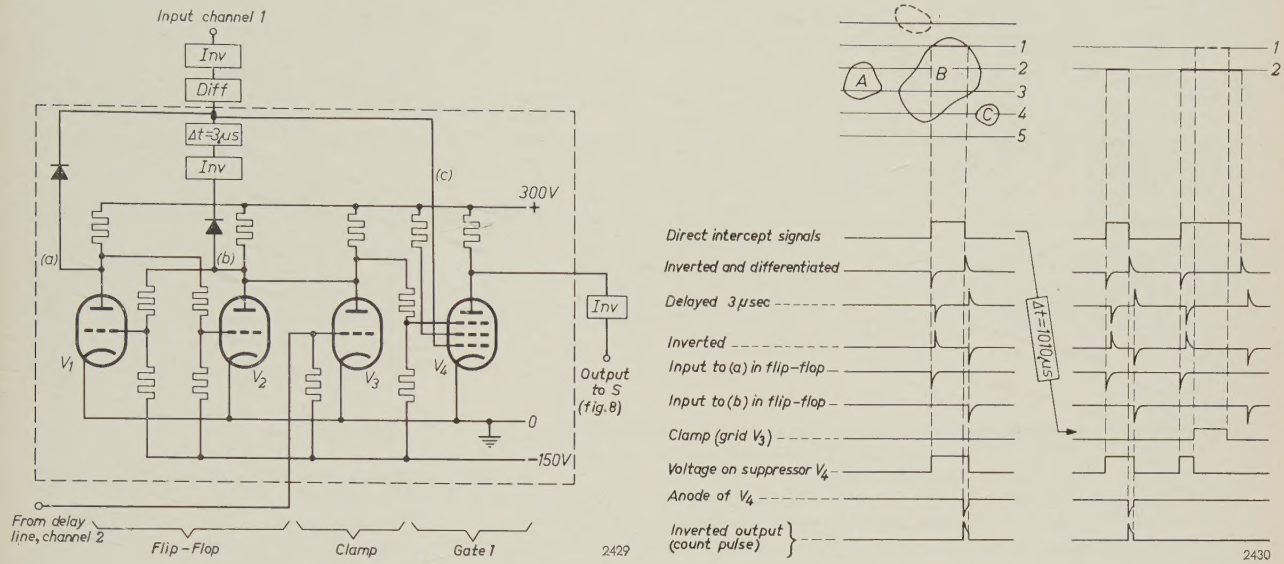

a *b* *c*

Fig. 8. *a*) Count-pulse generator (channel *1* in fig. 7) consisting of flip-flop, clamp and gate. The incoming shaped intercept signal is inverted and differentiated. The two peaks corresponding to leading and trailing edges are then fed to the three inputs *a*, *b* and *c* of the circuit. In the quiescent state (no intercept signal), V_1 is cut off and V_2 is conducting, so that V_4 is cut off.
b) Waveforms at various points during scanning of the line marked *1*, when the *first* intercept of a particle *B* occurs.
c) Waveforms during line *2*, when the first intercept of *A* occurs and the *second* intercept of *B*. Owing to the presence of the overlapping clamp pulse, delayed from line *1*, the line *2* count pulse of *B* cannot pass gate *1*. Likewise, on the succeeding lines, neither *A* nor *B* can be counted again. In line *4* the particle *C* will be counted since it is not overlapped by *B* in the *previous* line of scan. The dotted particle is drawn in the critical position of zero overlap with respect to *B* (see text).

intercept signal from the previous line via channel *2*, delayed by 1010 μsec (the total line scan period). It is here that the "overlap" criterion (see p. 255) is introduced. Normally, during the *first* intercept of any particle, there is no delayed pulse emerging from the 1010 μsec delay line. Hence the flip-flop remains unclamped and is triggered by the negative-going pulse corresponding to the leading edge of the intercept (fig. 8*b*). In this state the flip-flop applies a potential to gate *1* which opens it to positive pulses. The flip-flop is reset by the delayed (3 μsec) and inverted pulse corresponding to the trailing edge of the intercept. The 3 μsec delay makes sure that the count pulse has time to pass through the gate, and In the former case the negative (leading edge) pulse is unable to trigger the flip-flop and gate *1* remains closed. In the latter case the flip-flop is operated and the gate opened but before the count pulse (trailing edge of intercept) arrives, the clamping pulse has already returned the flip-flop to its initial state and therefore closed the gate. In neither case, therefore, does the count pulse pass gate *1*. Only on the first intercept of each particle does the count pulse pass through to the counter, giving only one count per particle, as required.

Now suppose there is an adjacent particle (dotted in fig. 8*b*) intercepted by the line previous to the first line of scan (*1*) of a given particle (*B*). This clearly

[15]) Used throughout this article in the sense that pulses can pass through a gate; when a gate is shut, the pulses are blocked.

[16]) Except in the case of a very slender particle making an angle of less than 45° with the scan direction.

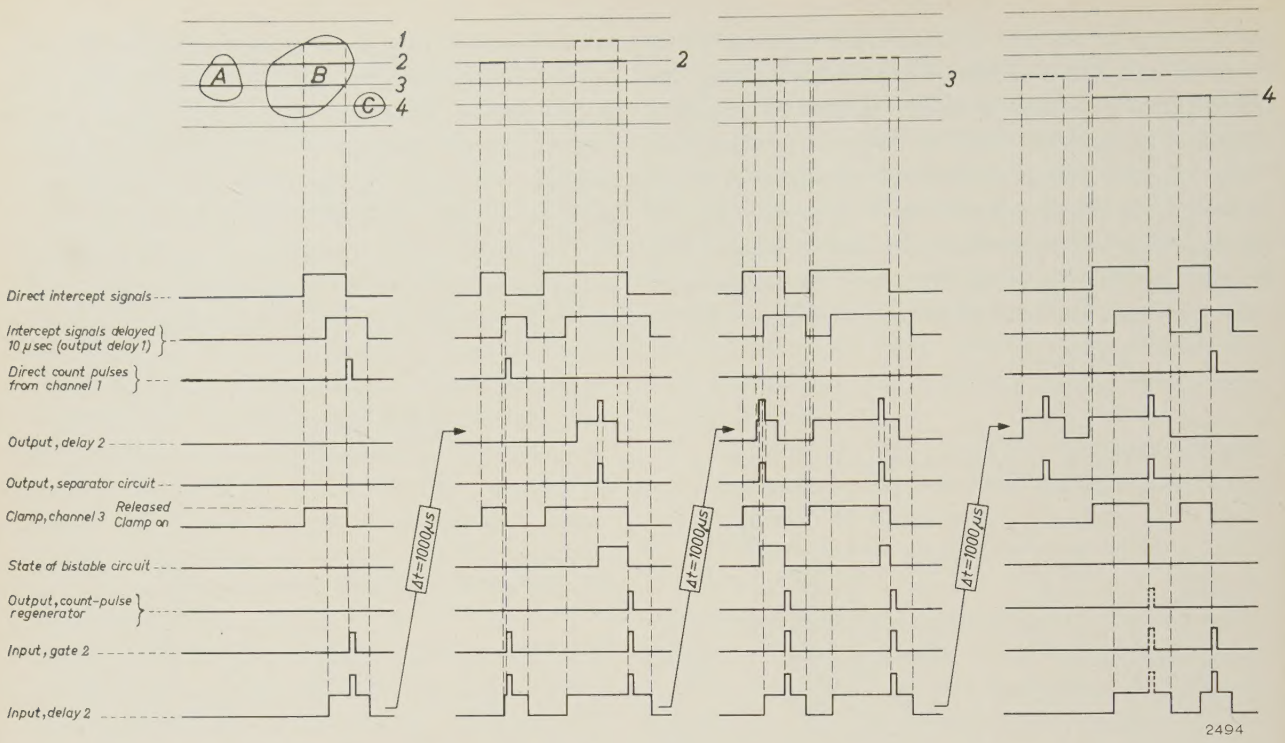

Fig. 9. Waveforms illustrating the regeneration and recirculation of count pulses. Portions of four lines of scan are shown, side by side, covering the three particles *A*, *B*, *C*. Note that delay *2* delays the pulses by 1000 μsec, that is, 10 μsec *less* than the line-scan period.

Between lines *3* and *4* the shape of the exit-edge of particle *B* is such that the clamping pulse in channel *3* barely overlaps the recirculating count pulse of this particle. The bistable circuit in channel *2* is therefore only just — or just not — triggered, so that the count-pulse regenerator may not always emit a regenerated count pulse (dotted in column *4*). This gives rise to negligible sizing errors, however, since the maximum intercept of most particles occurs before such an exit-edge is encountered; any particle greater than the pre-set size has then already been counted and its count pulse has ceased to recirculate.

gives a delayed clamping pulse close in time to the first direct intercept pulse from *B*. Provided that there is no actual overlap of these two pulses, the above circuitry correctly interprets *B* as a new particle and makes a count. If, however, the pulses overlap, *B* would be interpreted as an extension of the particle shown dotted. Only one count would thus be made for the two particles.

In counting, the mercury delay line carries only two sets of signals, viz. the intercept signals from channel *2* (fig. 7) and the time-base synchronizing pulses (see later). The separator circuits following this delay line (see below) simply route the delayed intercept signals to the count-generator clamp and separate out the synchronizing pulses for the scanner time-base; only during sizing is there a third set of pulses ("count" pulses in the recirculation circuit, bold lines in fig. 7) to be routed by the separator circuits. We now consider the sizing operation.

Sizing

For measuring the size distribution of a particle sample, the switch *S* is placed in the left-hand position ("Size") as drawn in fig. 7. All four channels of fig. 7 and also the recirculation circuit (bold lines) are now operative. The trailing edges of all intercept signals generate "count" pulses in channel *1* but, again, only the *first* count pulse of each particle passes gate *1*. With *S* as drawn, each such pulse (length 3 μsec) now passes via a diode to gate *2*, which is normally open. It then enters the 1000 μsec delay line, being superimposed upon the shaped intercept signal, itself delayed by 10 μsec (*fig. 9*). After separation from the intercept and sync pulses (see later), the count pulse passes to a bistable circuit (flip-flop) (fig. 7), which it triggers provided that the clamp has been released by the leading edge of a direct intercept signal to the clamp via channel *3*. (A direct intercept signal is always present except during the scanning line *following* the last intercept of a particle; what happens then we shall see presently.) The bistable circuit remains in its triggered state until reset by the re-application of the clamp at the end of the intercept signal.

When the bistable circuit resets, a differentiating circuit produces a pulse which is shaped to form a regenerated count pulse. Gate *3* being normally closed, this count pulse again passes (now via diode

d_2) to the gate *2* (normally open) and hence recirculates round the path shown in bold lines in fig. 7. Trains of count pulses, having originated at the first interception of each particle and being regenerated once per circulation, are therefore circulating continuously round this path while the corresponding particles are being scanned. Each count pulse continues to recirculate until the length of an intercept pulse of the associated particle exceeds a certain pre-set value, when gate *2* is momentarily shut and gate *3* simultaneously opened; this particular count pulse then passes to the counter via *S* and its recirculation ceases. This action is performed by the sizing discriminator (channel *4*), to be described presently.

If, however, the first or succeeding intercepts of a given particle never reach the pre-set pulse length, recirculation of the count pulse is stopped when the scan of that particle is complete, and it is not allowed to proceed to the counter. This is achieved by the clamp in channel *3*, mentioned above. The count pulse of the undersize particle, initiated at the first intercept, is recirculated (and regenerated) during each line of scan in the manner described above. After the last scan of the particle, however, there is no direct intercept signal in channel *3* to release the clamp on the bistable circuit at the moment that the delayed count pulse arrives. For this reason the bistable circuit cannot be triggered by the incoming count pulse. Since it is not triggered, there is also no reset and hence no regenerated count pulse is passed on. Recirculation therefore ceases and the undersize particle is not counted.

We must now examine how the instrument discriminates between particles greater than the pre-set size and those smaller. The pre-set signal length is chosen by setting a potentiometer in the discriminator in channel *4* (fig. 7). The discriminator (*fig. 10a*) consists of two parts: (i) a Miller linear ramp generator driven by the direct intercept signals, and (ii) a Schmitt trigger circuit acting as a pulse amplitude discriminator. The former is a Miller integrator circuit in which the charge and, therefore, the voltage on a condenser is made to depend linearly on the time for which the intercept signal is present at its input. A pulse *amplitude* discriminator can thus be used to discriminate between intercept signals longer or shorter than a given pre-set value. This value is set by means of a potentiometer which controls the grid bias of the input valve of the Schmitt trigger circuit. As will be clear from the waveforms in fig. 10*b*, the latter emits a square pulse whenever the Miller voltage exceeds the pre-set value necessary to trigger it. This is the case whenever a direct intercept signal is longer than the pre-set value. The duration of the pulse from the

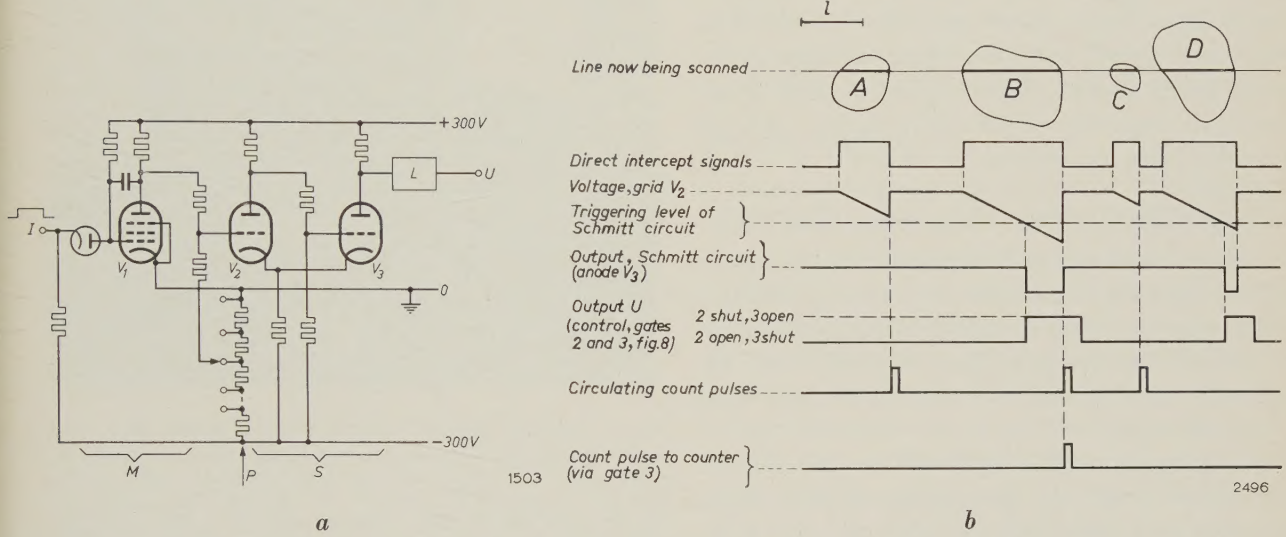

Fig. 10. *a*) Sizing discriminator circuit (simplified). Direct intercept signals are fed via channel *4* (fig. 7) to the input *I* of the Miller integrator *M*, and cut off the diode for the duration of each signal. The anode voltage of V_1 is linearly dependent on the duration of each signal. At a certain value of the grid voltage of V_2, set by the size pre-set potentiometer *P*, the Schmitt circuit *S* is triggered. The pulses at the output *V* are lengthened by 8 μsec by a monostable flip-flop *L*.
b) Waveforms during the scanning of part of a line. Four typical particles are shown. With the potentiometer set for the particle size *l* indicated, *A* is too small to be counted but will be counted in the next line of scan; the *B* intercept is greater than the pre-set size, so that *B* is counted; particle *C* is too small and will not be counted; the *D* intercept is greater than the pre-set size, but this particle has been already counted in a previous line, so that its count pulse has ceased to recirculate.

Schmitt trigger is governed by the time for which the Miller voltage remains above the pre-set value, i.e. until the end of the direct intercept signal; however, the Schmitt circuit is followed by a monostable flip-flop which adds a further 8 μsec to the length of this pulse. In this way the pulse emitted from the discriminator overlaps by some 8 μsec the trailing edge of the corresponding intercept signal. The discriminator output pulse passes to gate *2* which it shuts and gate *3* which it opens. Hence the recirculating count pulse of this particle (which has just been regenerated by the reset action of the signal via channel *3*) ceases to recirculate, but passes via gate *3* to the counter.

It will be clear that for the correct functioning of the circuits it is essential that the total line-scan period (scan + flyback periods) always remains exactly equal to the total delay provided by delay lines *1* and *2*, viz. 1010 μsec (nominal); if it were not, the delayed signals would not always be correctly phased with respect to the next line of scan. It is therefore necessary to lock the line time-base to the actual delay period. This is done by passing the time-base triggering pulses (sync pulses) through the delay lines, as outlined presently.

Further details of various components and circuits

Having described the essentials of the equipment and how it counts and sizes, we now go back to consider the design and operation of one or two of its critical units, in particular the delay line, the separator circuits and the time-bases and their synchronization.

The complete instrument with covers removed is pictured in fig. 11; the location of some of the sub-units is given in the caption.

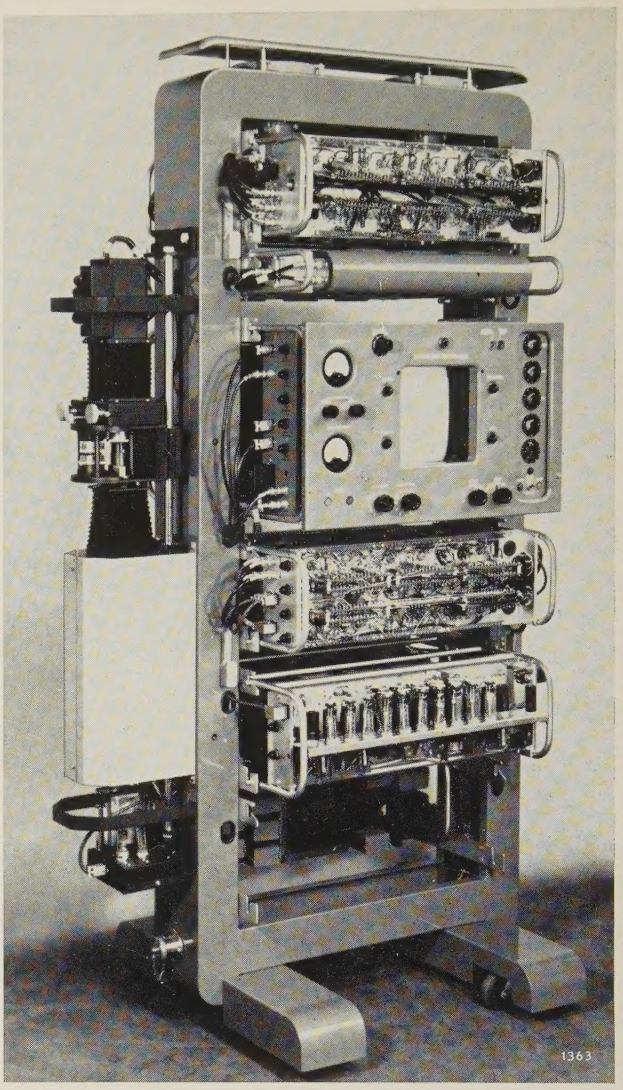

Fig. 11. Complete instrument with covers removed. On the left is the flying-spot scanner. The scanning tube is concealed by a screen (left). Between the two bellows can be seen the two alternative projection lenses (cf. fig. 5). The units visible are, from top to bottom: video chassis, containing intercept-pulse shaper and amplifier, count-pulse generator and delayed intercept-pulse separator circuit; mercury delay line and associated circuits, including sync-pulse separator; display panel; line and frame time-bases and synchronizing circuits; power pack.

Scanning raster, resolution and bandwidth requirements

In planning the instrument it was decided that the smallest particle to be measured should have a diameter of 1% of the line-scan length. This gives a sufficient resolution for most applications. For the resolution in the vertical sense, assuming a square field, a minimum of 100 lines is indicated.

The frequency of frame scanning should not be too low, otherwise display difficulties will be encountered. On the other hand it should not be too high, otherwise expensive high-speed logical circuits will be required to be able to cope with the above-mentioned resolution. With a 100-line raster, a frame frequency of about 10 c/s was chosen; the flicker of the display is then not excessive and focus and clipping adjustments can be made reasonably rapidly [17]). The line-scan period is 1010 μsec, as mentioned earlier; allowing a 30% blanking period for flyback and edge blanking, the active trace period is 700 μsec, making the smallest element to be resolved 7 μsec (1% of picture width). The signal channels (photomultiplier, video amplifier, switching circuits, delay line) must therefore be able to handle pulses of 7 μsec without introducing excessive distortion.

The requirements of the flying spot on the scanner tube are: *a*) small enough spot to give the required

[17]) A later version of the instrument employs a 120-line raster and a frame frequency of ~7 c/s.

resolution, and *b*) sufficient light output. The effective diameter of the spot depends on the tube beam current and the photomultiplier clipping level (*fig. 12a*). With the MC 13-16 tube and the gain employed the effective spot diameter d is about 0.3 mm on the screen. The raster being 60 × 60 mm, the spot represents about 0.5% of the active line scan and is therefore small enough to resolve the smallest particles (1% of line scan). Assuming that the intensity of the spot is constant over its effective diameter d,

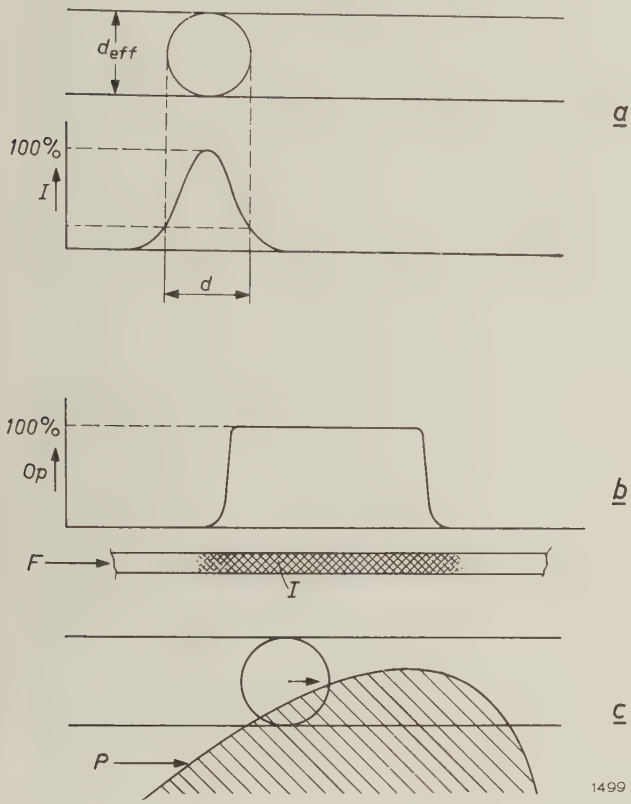

Fig. 12. *a*) The effective diameter d_{eff} of the scanning spot varies with the scanner-tube beam current and the photomultiplier gain, owing to the non-uniform intensity profile of the spot.
b) Percentage opacity *Op* of a particle image *I* in the photographic film *F*.
c) Oblique encounter of scanning spot with a particle edge *P*.

the rise time τ of the video intercept signal when the spot crosses a particle edge (assumed perfectly sharp and perpendicular to the direction of scan) is

$$\tau = td/l,$$

where t is the period of the active line scan and l its length. With $t = 700$ μsec and $l = 60$ mm, we find $\tau = 3^1/_2$ μsec. The video amplifier system was therefore to be designed so that pulses with rise times of rather less than this (2 μsec) pass through with little deterioration while not allowing excessive noise to pass. The theoretical bandwidth required [18]) is

$$\beta \approx 0.4/\tau = 0.4/(2\times 100^{-6}) = 200 \text{ kc/s}.$$

Final trimming of the amplifier stages was done empirically, using a test sample photographically reproduced from drawings.

The rise-time of the particle intercept signals is in general somewhat longer than the figure given above for the following reasons:

a) the intensity of the spot is *not* constant over its effective diameter as assumed above; moreover the effective diameter varies somewhat with fluctuations in the photomultiplier and amplifier system (fig. 12*a*);
b) the edge of the photographic image of each particle has a certain opacity profile (fig. 12*b*);
c) in general the particle edge is met obliquely by the scanning spot (fig. 12*c*).

As regards the spot brightness, the permissible energy in the raster is related to the area of the tube face actually scanned. With 100 lines, each of about 0.3 mm width, the area covered is effectively only about 50% of the 60 × 50 mm raster. The tube is therefore run at 20 to 50 μA (max.) beam current, i.e. about 50% of its rated value. This gives sufficient light, while helping to ensure a small spot diameter.

Mercury delay line

The mercury acoustic delay line [19]) consists of a sealed rectangular tank of mild steel (*fig. 13a*) about 2 cm deep, filled with mercury (filled under vacuum to exclude all air and water-vapour). Identical quartz crystal plates (X-cut) mounted at the 45°-bevelled corners, function as transmitting and receiving elements. Each plate, vibrating in the thickness-compression mode and operating at a wavelength very small compared to its diameter, has a polar diagram with a very narrow main lobe (first minimum at ~ 0.7°). With such a narrow ultrasonic beam and such an angularly-selective receiver it is possible to allow the beam to make multiple reflections at the walls before arriving at the receiver crystal. This makes for a compact delay line. Fig. 13*b* shows the path of the main beam.

To reduce the small amounts of coherent sound energy reaching the receiver via other paths (e.g. signals emitted by the side lobes), the regions of the walls between the reflection points of the main beam are grooved, so that local specular reflection is prevented. Unwanted ultrasonic radiation is therefore scattered, destroying any phase coherence. Spurious signals originating mainly in the side lobes are thereby largely eliminated.

---

[18]) See, for example, G. E. Valley and H. Wallman, Vacuum tube amplifiers, p. 80 (Rule 4), M. I. T. Radiation Laboratory Series, Vol. 18, McGraw-Hill, New-York 1948.
[19]) C. F. Brockelsby, Ultrasonic mercury delay lines, Electronic and Radio Engr. **35**, 446-452, 1958.

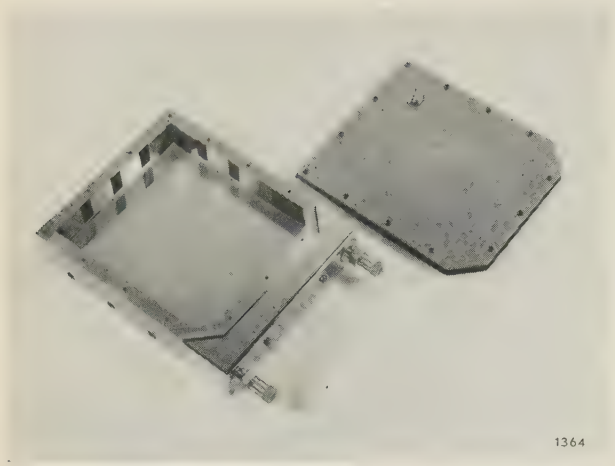

a

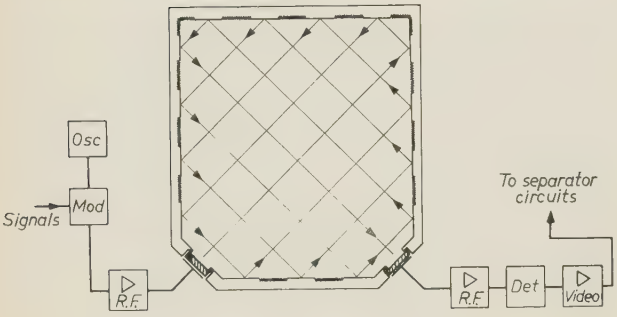

b

Fig. 13. *a*) Photo of delay-line tank. Internal dimensions 115 × 102 mm.
b) Sketch of delay line with associated units. The transmitted beam undergoes 15 reflections before arriving at the receiver crystal. Between the points of reflection, the walls of the tank are grooved (angle of groove ≠ 90°) to scatter any off-beam coherent radiation.

Another source of spurious signals is that portion of the sound energy of the main beam which is reflected by the receiver crystal, returns to the transmitter and is reflected back to the receiver again. These "third-time-round" signals (with 3× the normal delay) can be reduced to negligible amplitudes by tilting the receiver crystal through an angle Θ (rather more than 0.2°) from its optimum position. This causes only a slight reduction in the sensitivity to the main beam, but the third-time-round sound is incident at an angle 3Θ ($\approx 0.7°$), an angle that corresponds to the first minimum of the receiver polar diagram. The exact angle of tilt of the receiver crystal necessary to obtain the maximum attenuation of the third-time-round signals is found by trial and error.

The quartz crystals have a natural frequency of 10 Mc/s. Owing to the attenuation of the ultrasonic waves in mercury, the frequency characteristic of the delay line peaks at about 7 Mc/s, and this is chosen as the frequency of the carrier wave. The signals are modulated on this carrier and fed to the transmitting crystal via a power amplifier. At the receiver the signals from the crystal pass via an R.F. amplifier and detector to a video amplifier. From here they pass to the channel-separating circuits (*fig. 14a*).

Channel-separating circuits

There are three sets of pulses passing simultaneously through the delay line: particle intercept pulses, "count" pulses and synchronizing pulses for the flying-spot time-base (fig. 14b). These are identified as follows. The "count" pulses are always superimposed on the intercept signals, as we have seen; selection between these signals can therefore be achieved by amplitude discrimination. The synchronizing pulses are separated in time from the other signals in that they occur during a period in which the line scan is blanked off. The blanking pulse for this purpose is obtained from two monostable flip-flops operated by a Schmitt trigger circuit which forms part of the line time-base and synchronizing circuits; see next section. This blanking

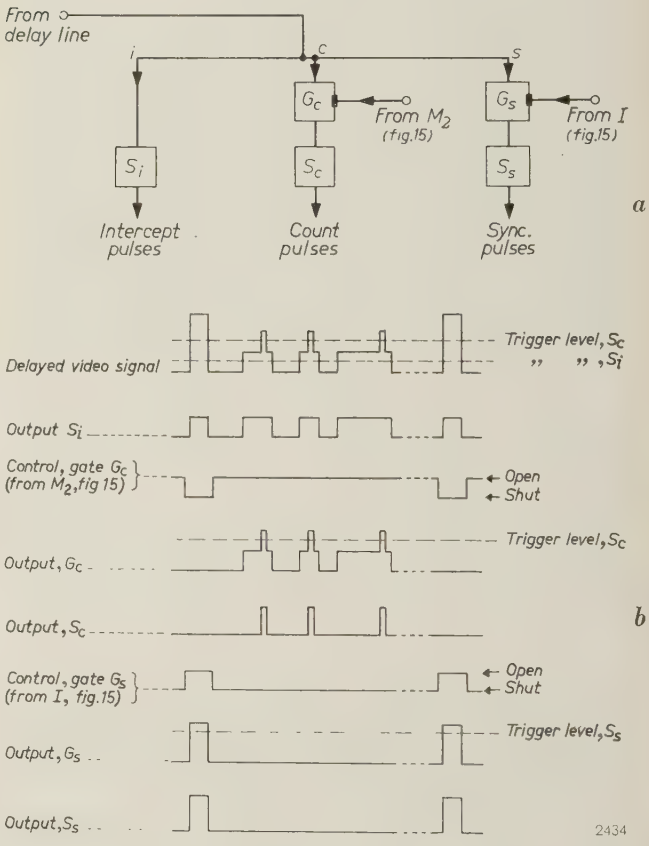

Fig. 14. *a*) Block diagram of channel-separating circuits. *i* intercept channel, *c* count-pulse channel, *s* sync-pulse channel. *G* are gates, and *S* Schmitt trigger circuits.
b) Waveforms in the three channels. In channel *i*, besides the delayed intercept signals, there are sync pulses. The fact that sync pulses are also fed to the clamp of the count-pulse generator does not matter because the scanner is blanked off when the sync pulses arrive. Channel *c* is blocked to sync pulses by the scanner blanking pulse which shuts gate G_c. Channel *s* is blocked to count pulses by the inverse of the scanner blanking waveform: gate G_s is thereby shut during the active scanning period.

pulse also shuts gate G_c in fig. 14*a* during the interval indicated in fig. 14*b*. This means that no sync pulses can enter the count-pulse channel (No gate is necessary in the intercept-signal channel as the sync pulses are present only during the blanked-off period, when there are no intercept signals; their arrival at the clamp in channel *1* (fig. 7) is then of no consequence.) The inverse of the blanking pulse is used to shut the gate G_s during the *active* scanning period (~700 μsec), so that no count pulses can enter the sync channel.

This completes the measures necessary to separate the signals of the three channels.

The sync-pulse amplitude is slightly greater than that of the count pulses and represents in fact the peak carrier amplitude; this is used as a datum level for the automatic gain control in the R.F. amplifier. ("peak white" in television systems with positive modulation).

Time-bases, synchronization and blanking waveforms

The line time-base is a Miller integrator linear-ramp generator, in which scan and flyback voltages are initiated by a Schmitt circuit. The free-running time of this arrangement is made somewhat greater than the required total line period and the Schmitt circuit is triggered by its own output pulses delayed in delays *1* and *2* (fig. 7). In this way the line time-base is synchronized with the actual total delay, so that variations in the delays (especially in the mercury delay line, which is temperature-dependent) cannot affect the phasing between direct and delayed signals.

The frame-scan time-base is also a Miller integrator triggered by a Schmitt circuit. The frame period is here determined by the free-running time of the circuit or, in later versions of the instrument, by a counting circuit which locks the frame period to a specified number of lines (see note [17]).

The waveforms for the scanner blanking (spot suppression) and for the channel separator circuits are produced by two monostable flip-flops in cascade The first of these (M_1, *fig. 15a*) is fed with the flyback pulses from the Schmitt circuit of the line time-base. The leading edge of these pulses triggers M_1, which returns to its original state after an interval of about 250 μsec. Differentiation produces a negative pulse which thus lags the end of the flyback by about 50 μsec. This sharp negative pulse triggers the second flip-flop M_2, which has a relaxation time of about 700 μsec. As may be seen from fig. 15*b*, the output of M_2 gives square negative pulses of about 300 μsec duration, separated by intervals of about 700 μsec (their total is of course equal to 1010 μsec).

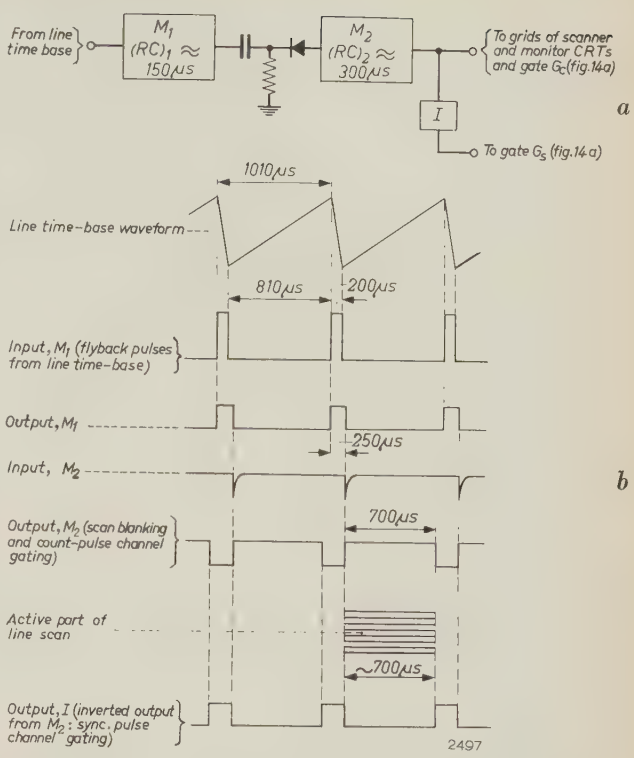

Fig. 15. *a*) Two monostable flip-flops connected in cascade are used to produce the scan-blanking and sync-strobe waveforms, as shown in (*b*).

These pulses are applied to the grids of the scanning and monitor tubes to suppress the spot during flyback and for a small portion of the line period at either extremity. The pulses are also applied to the count-pulse gate in the channel-separating circuits (G_c in fig. 14*a*), so that the sync pulses are denied entry to the count-pulse channel.

The inverse of the above waveform is applied to the sync-pulse gate in the channel-separating circuits (G_s in fig. 14*a*). The pulses shut gate G_s during the active scanning period, thus preventing count pulses from entering the sync channel.

Calibration and performance

The eleven settings of the sizing potentiometer correspond to *nominal* sizes from 0.20 to 6.40 mm. In order to have a check on the absolute sizes, and also to facilitate initial adjustment of the instrument, it is desirable to use a calibration sample such as the wedge shown in *fig. 16a*. This is easily prepared by making a drawing of known dimensions, and reducing it photographically on to 35 mm film. With the sizing potentiometer on the central size (1.14 mm, bold arrow in fig. 16*a*), the clipping level of the video pulse shaper (fig. 7) is adjusted till the displayed image at this point is just tagged (cf. fig. 6), i.e. just counted. The sizing potentiometer is

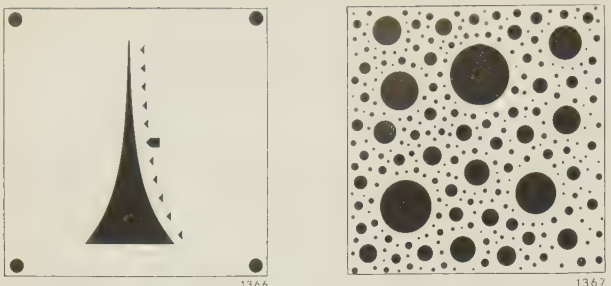

a *b*

Fig. 16. *a*) Calibration wedge, the width opposite each arrow increasing by a factor $\sqrt{2}$ between one arrow and the next. *b*) Test sample of circular spots whose size distribution is known. Both (*a*) and (*b*) represent a field of 20 × 20 mm on the actual negative. (For these samples and the calibration procedure described in the text we are indebted to Mr. W. A. Welling, Royal Dutch Shell Laboratories, Amsterdam.)

then set at the smallest range (0.2 mm) and the photomultiplier gain adjusted until only the image above the first arrow is tagged in the display. The adjustment may be repeated if necessary to obtain the optimum settings.

Whilst the absolute accuracy of the sizing and counting functions of the instrument are dependent on the shape factor of the particles being analysed and on the sharpness and contrast of their photographic image, the repeatability of results obtained from samples of the same material is of a very high order. For particles of circular profile it is found that, due to the line width (i.e. spot diameter) and spacing, about 5% of those lying in the smallest size range (0.2-0.28 mm) will be missed. Repeatability can be checked by means of a test sample such as that in fig. 16*b*, representing a known size distribution.

Table I shows some results of a series of tests carried out with such a test sample (not the one illustrated) on an instrument which had been in service for one year. These results illustrate the repeatability of results when the instrument parameters are re-adjusted between consecutive analyses of the same test sample.

Fig. 17 shows a photograph of spray droplets formed by the break-up of a jet from a fan-spray nozzle. The droplet size analysis of such a photograph is shown in *fig. 18*; two sets of points are plotted, representing size distributions measured at

Fig. 17. Spray droplet photograph taken by a spark-photographic technique during the development of an atomizing system for liquid fuels. As reproduced here, the droplet spray appears at about actual size. The original negative scanned in the analyser had a magnification of 2× actual size.

Table I. Total count and size distribution of "particles" in an artificial test sample of known size distribution, as measured under various conditions. Each count represents the mean of 10 complete scans of the field.

Condition	Total count	Sizing: number of particles greater than d (mm) =										
		0.10	0.14	0.20	0.28	0.40	0.56	0.80	1.12	1.60	2.24	3.2
Actual number of particles in test sample	426	426	252	147	82	38	19	11	6	3	1	0
Initial state	426.0	400.2	250.9	143.9	82.0	38.0	19.0	11.0	6.0	3.0	1.0	—
20 minutes after switch-on	426.0	400.0	251.9	145.7	81.0	38.0	19.0	11.0	6.0	3.0	1.0	—
Photomultiplier gain changed slightly	425.9	388.9	243.0	142.9	80.6	38.0	19.0	11.0	6.0	3.0	1.0	—
Photomultiplier gain restored to initial value	426.0	390.1	245.0	144.6	81.1	38.0	19.0	11.0	6.0	3.0	1.0	—
Clipping level adjusted slightly	426.0	398.4	252.0	146.9	81.6	38.0	19.0	11.0	6.0	3.0	1.0	—

two slightly different positions on the same photograph. The fact that both sets of points lie almost on the same curve implies not only a substantially unvarying droplet size distribution but also a high degree of stability and reproducibility in the instrument.

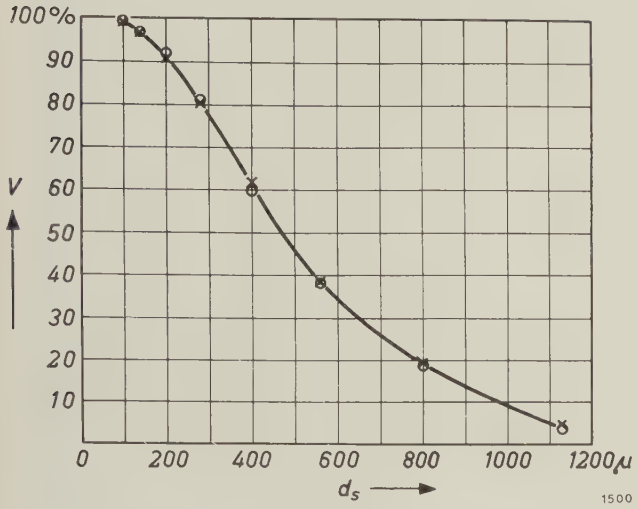

Fig. 18. Plot of two series of measurements of the size distribution of droplets from a fan spray nozzle using water at 25 pounds/inch². × Test A, sample field about 6 cm from nozzle. o Test B, sample field about 7 cm from nozzle. The counts are here plotted after conversion from a diameter size distribution to a volume distribution: V represents the total volume of all particles having diameters greater than d_s. (Photograph (fig. 17) and measurements by courtesy of Dr. J. D. Lewis, R. P. E., Ministry of Aviation, London.)

Summary. The problems involved in the automatic counting and sizing of particles are outlined in an introductory section to this article. Various possible scanning systems are described, together with some of the methods that have been used to avoid or allow for the effects of multiple or lumped counts. It is shown that flying-spot scanning together with some form of line-to-line signal association represent a very effective solution to the problem. For practical reasons line-to-line signal association can best be achieved by use of a line-to-line memory rather than by double-spot or guard-spot systems. Sizing can be conveniently performed by logical circuits that reject pulses shorter than a certain pre-set length. The following sections of the article describe the Mullard particle analyser. The sample is in the form of a 35 mm photograph (negative or positive) made from the original sample by direct photography, photo-micrography or electron microscopy. This greatly simplifies the optical arrangements and facilitates initial adjustments. With the aid of block diagrams and waveforms it is shown in detail how the instrument makes total counts and measures size distributions. The operation of some of the sub-units is explained with the aid of simplified circuit diagrams. Among the sub-units dealt with are the count-pulse generator, the sizing discriminator, the (mercury) delay line and the channel-separating circuits. The resolution is discussed in relation to the scanning raster and bandwidth requirements. The article concludes with a short section describing initial adjustments and calibration with artificial samples, and giving some results which demonstrate the reproducibility of the instrument.

A GAS-DISCHARGE INDICATOR TUBE FOR TRANSISTORIZED DECADE COUNTING CIRCUITS

by T. P. J. BOTDEN.

621.387:621.374.32

The problem of indication in transistorized decade counting circuits has long awaited a really satisfactory solution. The article below describes a gas-discharge decade indicator tube which responds to the small signals delivered by transistor circuits.

A scaling circuit, irrespective of whether it forms part of equipment for monitoring radioactivity or is a component of other counting equipment, obviously depends for its usefulness on being able to display in some way or another the result of a count.

In the case of equipment for monitoring radioactivity, for example, the pulses delivered by the radiation detector (e.g. a Geiger-Müller tube or a scintillation counter) are fed after amplification to a sequence of scaling circuits. With scale-of-two stages, the last stage is often followed by a mechanical register (which can handle no more than about 10 pulses per second); the state of the individual scaling stages can be seen from a neon lamp — lit or unlit — in each stage. Decade scaling circuits are usually equipped either with indicating neons — 10 per stage — or each stage consists of a decade scaler tube, which performs the dual function of scaling and indication — each tube thus indicating one digit of the number counted. Such scaler tubes may be either of the gas-filled type (decatron ring-electrode scalers) or of the vacuum type (decade scaler tube E1T).

Apart from giving a visual indication, as in a

mechanical register, scaler tubes thus form the primary functional elements of the circuit [1]). This means that the resolution of the first decade — which is the critical one — is determined by the tube; for the gas-filled tube this is about 300 μsec, and for the E1T tube about 30 μsec. The gas-filled type can therefore only be used where the highest counting rates are not required. In counting circuits from which an exceptionally high resolution is demanded, e.g. 0.1 to 1 μsec, the functions of scaling and indicating are again separated. The scaling is performed by vacuum-tube circuits (having a resolution down to 0.1 μsec) or perhaps by a "trochotron", a multi-electrode tube having a resolution of about 1 μsec [2]); the indication is provided by neon lamps or by numerical indicator tubes.

A resolving power almost as high as obtained with the best electron-tube circuits can be achieved with transistor circuits, which have the advantages of very compact construction and low energy consumption. Hitherto, however, the means of indication had presented difficulties inasmuch as a transistor circuit is unable to deliver a signal of sufficient amplitude to ignite a neon lamp or numerical indicator tube [3]). Moreover, a circuit of this type cannot provide the current needed to produce a clearly visible discharge without jeopardizing the counting operation. Further, in the case of decade scalers it is more convenient to have only one indicator tube for each decade. In this article we shall discuss a gas-discharge tube which provides an answer to these problems [4]). This tube, which is purely an indicator and does no counting, has an anode and ten cathodes arranged in a circle; the gas discharge can be shifted as required from one cathode to another by a signal of only 5 volts and less than 50 μA. The tube is not yet commerciably available.

Principle of the indicator tube

The structure of the tube is shown schematically in *fig. 1*. The face of a molybdenum ring K is coated with ten sectors of an insulation material (shaded in the figure). The ten sectors in between them each act as the cathode. About 5 mm above this ring there is a second ring A, of nickel wire, which acts as the anode. Above each of the ten cathodes can be seen a wire electrode T, the "trigger", by means of which the discharge is initiated at the desired place. The distance between the triggers and the cathodes is about 1 mm. *Fig. 2* illustrates some of the arrangements of cathodes and triggers; a photograph of a complete electrode system is shown in *fig. 3*.

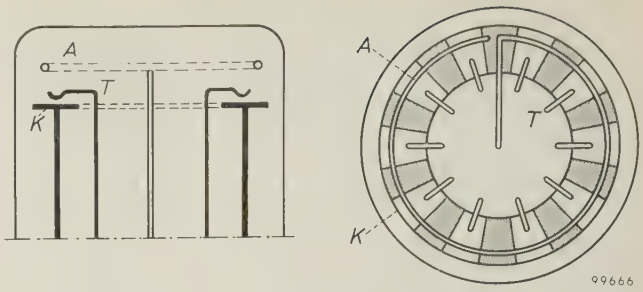

Fig. 1. Schematic representation of the indicator-tube electrode system. The surface of a molybdenum ring K is divided into twenty sectors. Ten are coated with a layer of insulating material (shaded), the other ten function individually as cathodes. The circular nickel wire A is the anode. Between the anode and each of the ten cathodes is situated an auxiliary electrode T, which functions as trigger electrode.

The tube is filled with neon gas to which 0.1% of argon has been added; the gas pressure is about 15 cm Hg. In order to obtain a clean cathode surface,

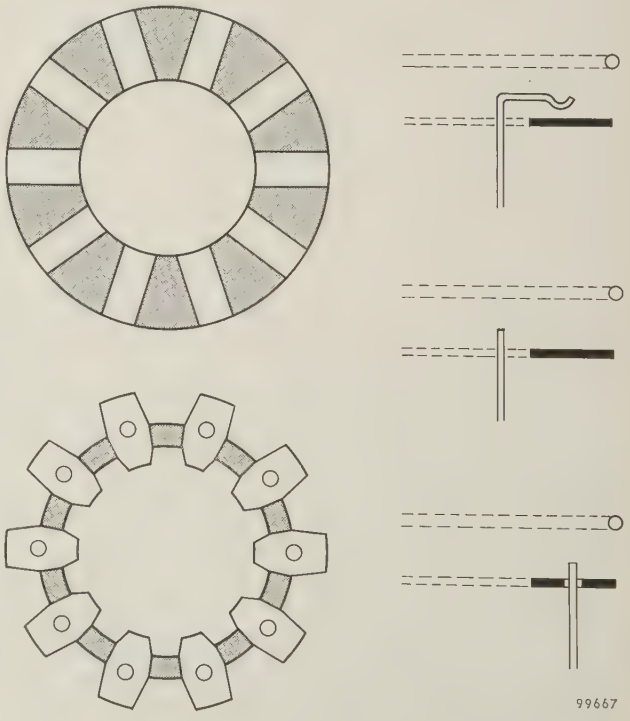

Fig. 2. Various arrangements of cathodes and triggers.

[1]) In ring-electrode scalers each count pulse causes a gaseous discharge between the disc-shaped anode and one of the ten cathodes arranged around it. The next pulse shifts the discharge to the adjacent cathode, and so on. Every time the discharge passes cathode number "zero", a pulse is delivered to the tube in the following scaling stage. (See e.g. R. C. Bacon and J. R. Pollard, Electronic Engng. **22**, 173, 1950 and G. H. Hough and D. S. Ridler, Electr. Commun. **27**, 214, 1950.)
The operation of the decade scaler tube type E 1 T has been described in this journal (A. J. W. M. van Overbeek, J. L. H. Jonker and K. Rodenhuis, Philips tech. Rev. **14**, 313-326, 1952/53).

[2]) See e.g. H. Alfven and L. Lindberg, Acta polytech. (El. Engng.) **2**, 106, 1949.

[3]) Cf. H. F. Stoddart, Nucleonics **17**, No. 6, 78, June 1959.

[4]) The development of this tube stemmed from an idea of M. van Tol of this laboratory.

the cathode is sputtered during manufacture [5]); the sputtered material on the glass wall helps to keep the gas uncontaminated. The reason for adding argon will be explained below.

The tube is fed with a rectified alternating voltage, which is not smoothed. A discharge is initiated when the amplitude of this voltage is sufficiently high. For a half-wave rectified supply, the supply voltage rises

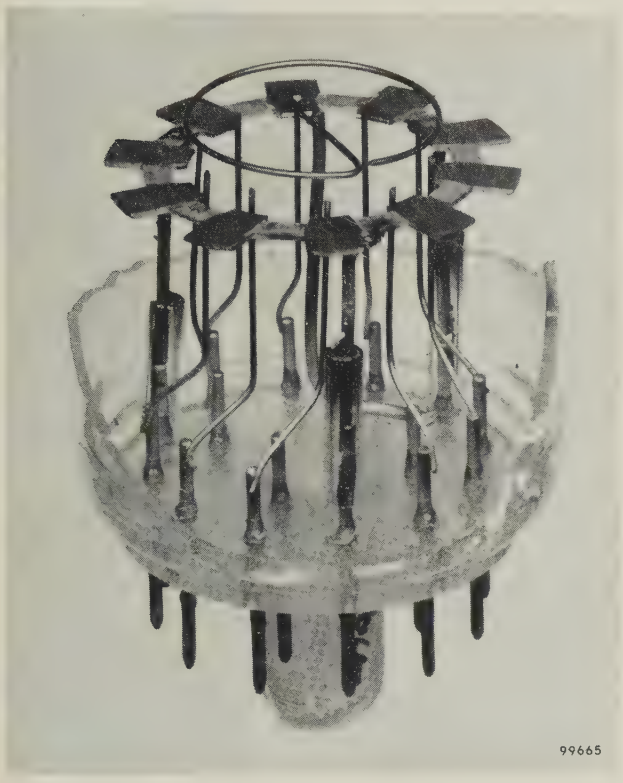

Fig. 3. An assembled electrode system.

to a maximum and drops to zero once in every mains cycle; the tube is therefore ignited and extinguished once per cycle. (However, a full-wave rectified voltage may also be used.) As can be seen from the circuit diagram in *fig. 4* (disregarding the blocks X_i for the moment), the triggers are at the same potential as the anode so long as there is no discharge. A discharge between the cathode and one of the triggers has a lower ignition potential than a discharge between cathode and anode, and therefore when the voltage begins to rise from zero a discharge first occurs between the cathode and one of the triggers. If the current produced by this auxiliary discharge is high enough — we shall return to this presently — the anode takes over the discharge almost immediately. The potential difference between cathode and anode then drops to the burning potential of the main discharge now occurring between these electrodes (a glow discharge), so that for the rest of that particular half cycle none of the other triggers can reach their breakdown potential. This process is repeated in every cycle of the mains frequency.

The place where the auxiliary discharge occurs can be selected by making the potential of the relevant trigger higher than that of the other triggers (and of the anode) by a small amount X. As a result this trigger reaches the breakdown potential earlier than the others and the discharge always recurs at the same position. If the voltage X is transferred to another trigger, the reignition in the next mains cycle will take place at that trigger, and so on. The periodic extinction of the discharge is thus essential in order to be able to displace the discharge from one position to another. It follows from the above that the tube can be "driven" with a signal whose amplitude is much smaller than the breakdown voltage itself. For the tubes made and tested by us, the amplitude of this signal was always less than 5 V.

A signal as small as this can readily be supplied by a transistor circuit. If the circuit is so designed that a signal X is applied to the trigger T_1 for a count of 1, to the adjacent trigger T_2 for a count 2, and so on, one can read from the tube the total result of a count. Evidently, it is immaterial whether or not the tube can follow a rapid counting operation because upon the next reignition after the completion of the counting operation the tube always burns at the position corresponding to the final result of the count. Since the power for the main discharge is not drawn from the transistor circuit, it is easy to ensure that this discharge will be sufficiently bright to provide a clear visual indication.

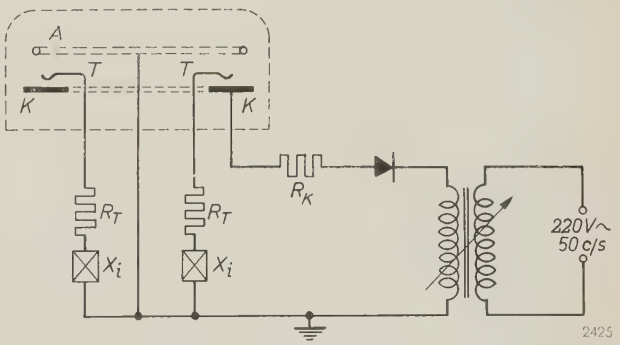

Fig. 4. Circuit diagram of indicator tube. A anode (earthed). K cathodes. T triggers. X_i voltage source providing the control signal. The current of the main discharge is limited by the resistor R_K, that of the auxiliary discharge by R_K together with one of the resistors R_T. The tube is supplied with a rectified alternating voltage (unsmoothed).

[5]) In this process the cathode is exposed for some time to intense ionic bombardment. Cathode material is thereby sputtered onto the inside wall of the glass envelope, where it performs the dual function of gettering and of preventing gas molecules in or on the glass wall from escaping. See e.g. T. Jurriaanse, Philips tech. Rev. **8**, 272, 1946.

As can be seen in fig. 4, the anode is earthed. This makes it possible to earth one of the two terminals of the voltage sources that supply the control signal (represented by X_i in fig. 4). In the practical application of the tube these sources are part of a transistor circuit.

Closer consideration of the gas discharge and the method of ignition

It has been shown in the foregoing that the operation of the tube depends, among other things, on the fact that a gas discharge can be initiated by a voltage lower than the normal breakdown voltage (but not, of course, lower than the burning voltage), and that this is done by producing an auxiliary discharge between the cathode and a trigger electrode. The extent to which the ignition potential of the main discharge is reduced depends on the current I_T of the auxiliary discharge. This is illustrated in *fig. 5* for one of the ten cathode-trigger positions and for a tube in which the pressure of the neon-argon filling was 14 cm Hg. It is seen that even for a trigger current I_T of only a few tens of μA the anode voltage V_a at which the main discharge is initiated is already much lower than the breakdown voltage measured in the absence of an auxiliary discharge. For maintaining the auxiliary discharge the current drawn from the transistor circuit need therefore only be, say, 50 μA (the figure mentioned earlier), which does not affect the operation of the transistor circuit.

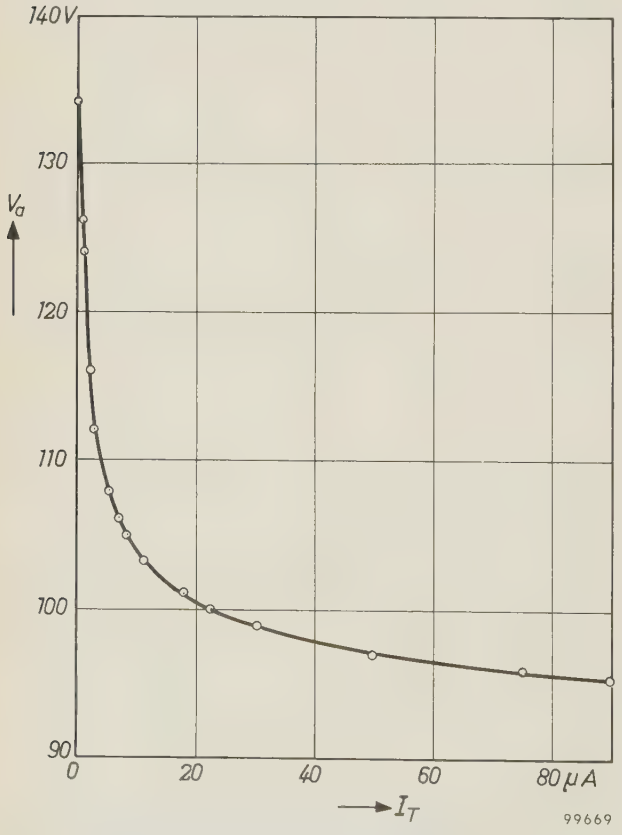

Fig. 5. Ignition potential V_a of the main discharge as a function of the current I_T of the auxiliary discharge for one of the ten cathode-trigger positions. The pressure of the gas filling (Ne + 0.1% Ar) was 14 cm Hg.

There are two reasons for the lowering of the ignition potential. In the first place, charge carriers (positive and negative) diffuse from the auxiliary discharge to the space between trigger and anode. Consequently, the current I_0 that begins to flow between cathode and anode when the supply voltage rises from zero is already, before ignition, greater than at the other cathodes. If this current exceeds a certain minimum value, the ignition voltage is no longer independent of it but decreases according as I_0 increases [6]). In the second place, the auxiliary discharge gives rise to a certain space charge (of positive ions) at the cathode. As a result the electrons in the space immediately in front of this cathode encounter more favourable conditions (a higher electric field) than those at the other cathodes for acquiring sufficient energy to ionize the gas atoms. At the other cathodes the field strength is determined solely by the applied voltage and the geometrical configuration [7]).

It should be noted here that the auxiliary discharge is neither a Townsend nor a glow discharge; the values of current and burning voltage are found in the descending transition region of the discharge characteristic between the two horizontal portions corresponding to the Townsend and glow discharge regimes (cf. *fig. 6*).

Factors determining the minimum value of the control voltage

If the potential difference V_d at which breakdown occurs between the trigger and cathode always had the same unvarying value for all trigger-cathode positions, the amplitude of the control signal could be extremely small. After all, this need not be much greater than the maximum difference found between the V_d values for the ten triggers. We shall now consider the factors that determine the actually occurring differences in V_d, and the measures adopted in the indicator tube to reduce them to a value lower than the 5 volts referred to above. First we shall recall the way in which a discharge is

---

[6]) For a brief discussion of the mechanism of this effect, see C. H. Tosswill, Cold-cathode trigger tubes, Philips tech. Rev. **18**, 128-141, 1956/57. See also M. J. Druyvesteyn and F. M. Penning, Rev. mod. Phys. **12**, 87-174, 1940.

[7]) See e.g. F. M. Penning, Electrical discharges in gases, Philips Technical Library 1957, Chapter VIII, or the article by Druyvesteyn and Penning quoted under [6]).

brought about, and the conditions to be fulfilled if the discharge is to be self-sustaining.

If a not unduly high voltage is applied across two electrodes in a gas-filled space, a minute current will

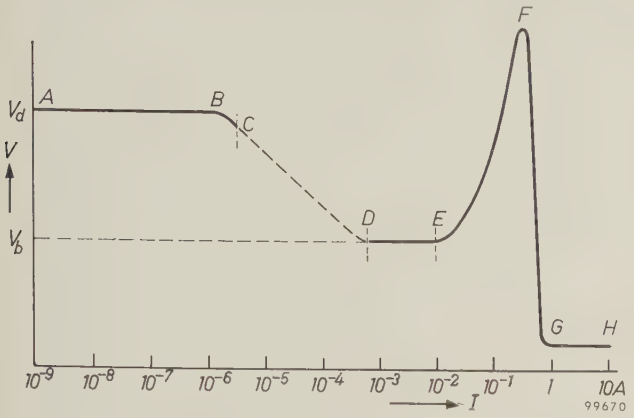

Fig. 6. Current-voltage characteristic of a self-sustained gas discharge. In the region AC of the Townsend discharge no space charge (of positive ions) has yet formed in the region AB, and the burning voltage is equal to the breakdown voltage V_d. A space charge begins to form in the region BC, and with rising current this continues into the region beyond C until at D the region of the normal glow discharge is reached (DE). Here too the burning voltage (which is now much lower than the breakdown voltage) is independent of I. The current density is likewise independent of I; as the current increases, a larger part of the cathode surface is covered, until at E the whole cathode is covered. A further rise in current causes the current density and the burning voltage to increase (anomalous glow discharge; EF). The region FGH is the arc-discharge region.

flow whose magnitude is determined by the number of charge carriers created per second by some external cause, such as cosmic radiation or the photo-electric effect of daylight. (If the tube is shielded from all radiation, the current drops to zero.) As the voltage is raised the current at first remains unchanged, then gradually increases and finally increases very rapidly, i.e. breakdown occurs. The gaseous discharge thus produced cannot be extinguished by suppressing the external cause that gives rise to the presence of the initial charge carriers; the production of charge carriers by the discharge itself—which is also the cause of the gradual increase of the current with rising voltage before the breakdown occurs — is now great enough to maintain the discharge. The charge carriers are generated both as a result of gas atoms being ionized by collision with electrons moving towards the anode (or trigger), and by ions reaching the cathode and liberating electrons from its surface. The discharge can remain self-sustaining if as many of these electrons are liberated from the cathode per second as are lost from the gas to the anode. The potential difference then required between cathode and anode (trigger) is equal to the breakdown voltage V_d (in the absence of any space charge).

If a voltage slightly higher than V_d is applied across the electrodes, nothing will happen until there is a free electron present at a suitable position in the space between the electrodes. Once such an electron exists, it will of course move through the electric field towards the anode. In doing so it ionizes gas atoms, as a result of which electrons are released which ionize other gas atoms, and so on. Because of the random character of the processes taking place in the gas and on the cathode, however, the "avalanche" thus produced may sometimes break off pending the arrival of a new initial electron. Not until the number of ions and electrons generated is extremely high is the chance of such an interruption eliminated. The time elapsing between the application of the voltage and the attainment of this situation is called the statistical delay. Since we are concerned here with random processes, this delay time may, in principle, have any value. The time elapsing subsequent to the formation of this stable avalanche up to the moment that the avalanche effect ceases to increase in strength is the "build-up" time of the discharge. At the beginning of this time interval there are already large numbers of ions and electrons present, and therefore the statistical fluctuations in the build-up time are extremely small and cannot be measured: the build-up time can thus be regarded as constant.

The condition that the discharge should supply its own electron requirements can be expressed by the equation:

$$\gamma(e^{\eta V_d} - 1) = 1. \quad . \quad . \quad . \quad . \quad . \quad . \quad (1)$$

Here γ is the average number of electrons released from the cathode by one gas ion, and η is the average number of electrons produced by each electron in the gas per volt of traversed potential difference. The value of γ depends on the velocity and kind of the ion and on the condition of the cathode surface. From (1) it follows that V_d depends on γ and on η.

Applying this to the new indicator tube, we may conclude that the differences in the γ value of the various cathodes are due solely to the condition of the cathode surfaces; the gas filling is of course the same in all cases. The surfaces of the ten cathodes are cleaned during manufacture by the sputtering process referred to, thus considerably reducing the differences in the γ value. The gettering action of the sputtered molybdenum on the glass wall helps to keep the gas clean and thus maintains this favourable situation over a very long time. Another fortunate circumstance is that V_d does not depend very markedly on γ. This can be understood from

the following reasoning. In the left-half of equation (1) the exponential term is $\gg 1$. To a good approximation we can thus reduce (1) to

$$V_d = -\frac{1}{\eta} \ln \gamma. \quad \ldots\ldots \quad (2)$$

The breakdown voltage, then, varies in proportion to $\ln \gamma$. Since $\ln \gamma$ varies only slowly with γ, the minor differences in γ that still exist after the cathode has been sputtered have scarcely any effect on V_d.

It also appears from (2) that V_d depends more strongly on η than on γ. Now η is by no means constant; its value depends on the ratio of the electric field strength E and the gas pressure p. For a given electrode configuration, E is inversely proportional, at a given voltage, to the linear dimensions of the electrodes, e.g. for two flat plates E is inversely proportional to the distance d between them. In this case, then, V_d is a function of pd (Paschen's law). *Fig. 7* demonstrates this relation for the breakdown of various gases between flat molybdenum electrodes [8]). It can be seen that V_d shows relatively little variation in a wide range of pd values in the case of a gas mixture of neon and 0.1% argon.

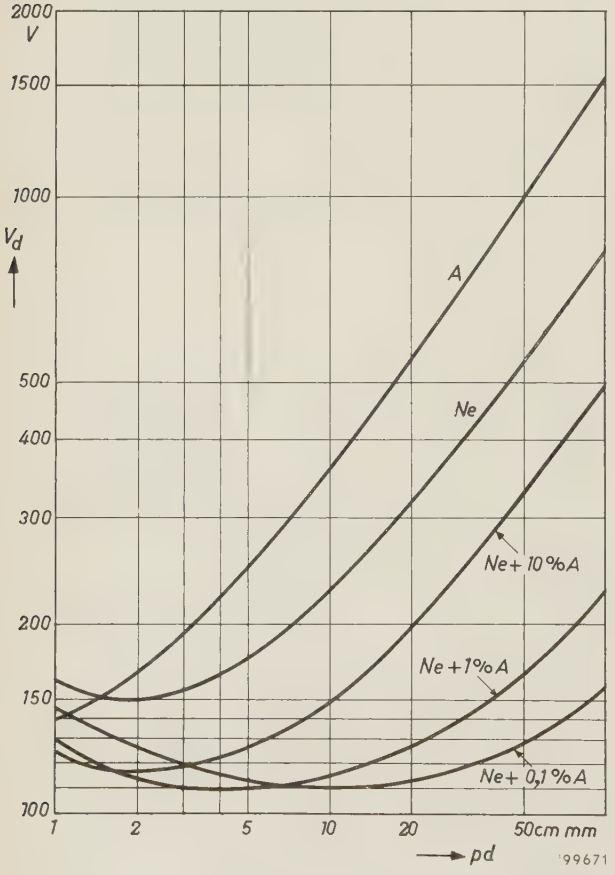

Fig. 7. Breakdown voltage V_d of various gases as a function of the product pd, using flat molybdenum electrodes (Paschen curves). For a mixture of neon and 0.1% argon there is relatively little variation of V_d over a wide range of pd.

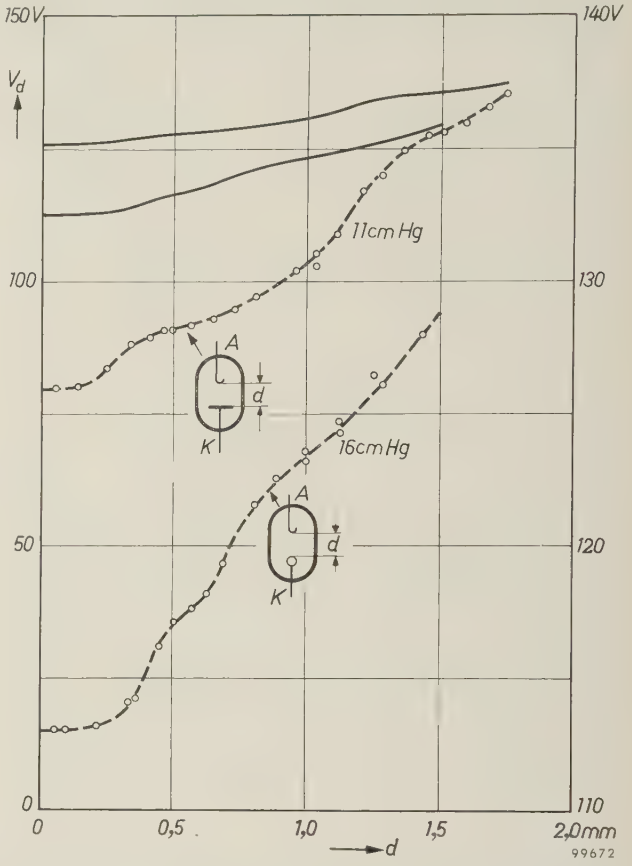

Fig. 8. Breakdown voltage V_d of a trigger-cathode combination as a function of the distance d between these electrodes (solid curves). The solid curve at the top applies to a flat molybdenum cathode, the lower one to a molybdenum-wire cathode. In the case of the flat cathode, V_d varies only by about 0.8 V per tenth of a millimetre for $d \approx 1$ mm. The gas pressure for the upper curve was 11 cm Hg, and for the other 16 cm Hg. The curves are derived from two series of measurements which are plotted as the dashed curves (V_d scale on right of figure).

Although the curves shown in fig. 7 do not entirely apply to the new indicator tube with its wire-shaped triggers, it was to be expected that here too, owing to the use of the Ne-Ar mixture, the ignition potential of the auxiliary discharge would not vary much with the electrode spacing. *Fig. 8* shows the results of an investigation into this question. In one series of measurements the trigger was mounted opposite to a flat molybdenum cathode, and in the other series opposite to a molybdenum-wire cathode. It can be seen that V_d does not in fact vary to any marked extent with d, and at very small d values it is virtually constant. With the flat cathode and $d \approx 1$ mm, V_d varies by about 0.8 V when d is increased or decreased by one tenth of a millimetre, i.e. by 10%. Thus, the choice of gas filling also helps to keep down the relative difference in breakdown voltage between the various trigger-cathode spaces.

[8]) S. M. Frouws, 3° Congr. Int. Fenomeni d'ionizzazione nei gas, Venice 1957, page 341.

Besides the condition of the cathode surface and the geometry of the electrodes there is a third factor affecting the minimum amplitude of the control signal. This is the phenomenon that, during operation of a given tube, the breakdown voltage V_d of any particular cathode-trigger position is not entirely constant, but shows certain fluctuations. As these are related to one of the delay effects mentioned above, and thus the magnitude of the fluctuations in V_d depends on the rate at which the trigger voltage rises, we shall defer the discussion of this subject to the following section, which deals with the relation between the minimum required signal amplitude and the properties (amplitude, frequency, waveform) of the supply voltage.

Voltage supply

As we have seen, for the purpose of shifting the discharge readily from one point to another the indicator tube is fed with a half-wave rectified

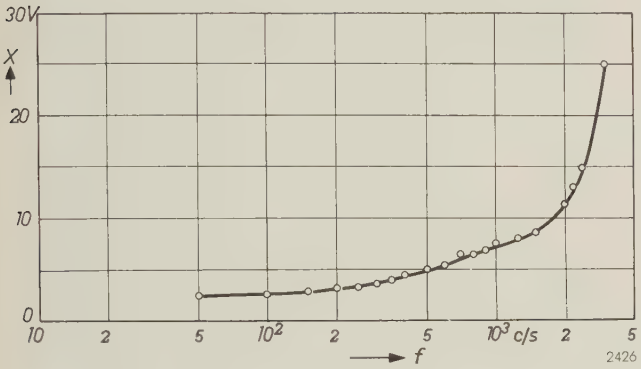

Fig. 9. The minimum required control voltage X as a function of the frequency f of the supply voltage. At frequencies above 3000 c/s, X is higher than 25 V (the difference between ignition and burning voltage) and therefore the discharge can no longer be displaced.

alternating voltage. For a visual indication the only requirement to be made of the frequency of this voltage is that the glow should not flicker. A frequency of 50 c/s is quite high enough for this purpose.

Investigation of the way in which the minimum required control voltage depends on the frequency of the supply voltage shows (see *fig. 9*) that the control voltage is substantially constant at frequencies up to about 300 c/s, but increases at frequencies higher than this. At frequencies above about 3000 c/s the discharge can no longer be displaced. The main reason for this is that, after the gas discharge is extinguished, all the ions and electrons constituting the plasma do not immediately disappear. If a voltage is again applied while there is still some residual plasma present, the ignition

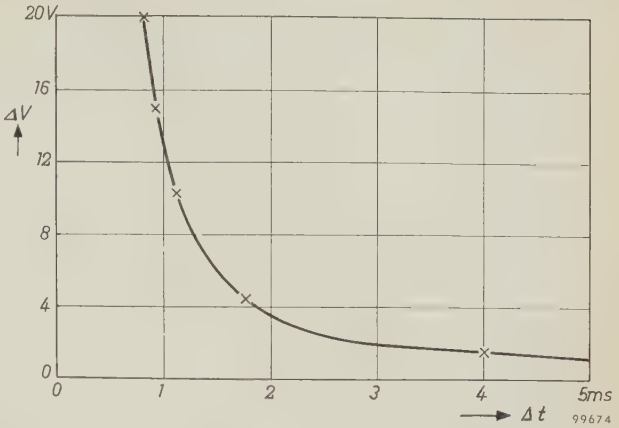

Fig. 10. The decrease ΔV of the ignition voltage (from the ignition voltage required when the tube has not been ignited for a long time) as a function of the time interval Δt between the moment a discharge is initiated and the moment at which the preceding discharge was extinguished. The smaller the value of Δt, the greater is ΔV. This is due to the fact that not all ions and electrons disappear immediately after extinction of the discharge.

takes place at a lower potential than otherwise. The drop is greater the greater the residual plasma density, that is to say, the shorter the time Δt between the extinction of the discharge and the re-application of the voltage. If the drop is such that the breakdown potential has fallen to the level of the burning voltage, the tube will always ignite at the same place. *Fig. 10* shows the result of a series of measurements performed to determine the drop in breakdown voltage on an indicator tube of the type described here. It is seen that for $\Delta t = 1$ msec, the decrease ΔV in the breakdown voltage amounts to as much as 13 V, and increases rapidly for even shorter times. This roughly agrees with the measurements given in fig. 9. The difference between the normal ignition voltage and the burning voltage (about 25 V) corresponds in fig. 10 to a Δt of 0.7 msec; as regards the minimum trigger voltage required for displacement of the discharge, this corresponds to a maximum supply frequency of approximately 1000 c/s. In view of the fact that the experimental conditions in the measurements summarized in fig. 10 differed from those normally encountered, the agreement with the value derived from fig. 9 may be said to be satisfactory.

In order to obtain some quantitative information on the effect of delay phenomena, recordings were made of the current in the main and auxiliary discharges, and also of the total current in both discharges together, as a function of time after the application of the voltage. The circuit used for the recording is shown schematically in *fig. 11*. The objects of this investigation were to determine the values of the statistical delay, and also to discover the rate at which the auxiliary discharge builds up,

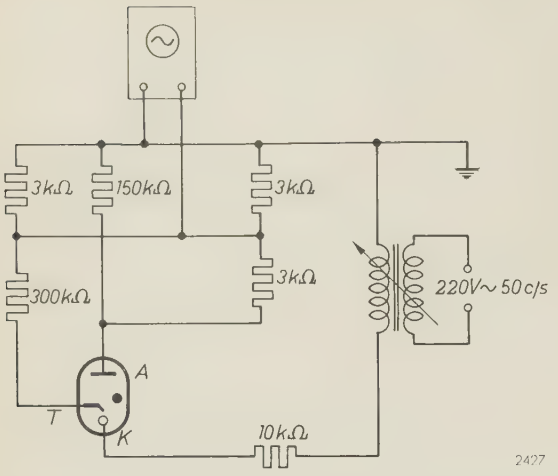

Fig. 11. Circuit for recording waveforms of the trigger current, the main current or the sum of certain selected fractions of each. The time-base period of the oscilloscope was chosen such that the full picture width corresponded to 30 μsec. A separate synchronizing circuit was dispensed with by triggering the time-base with the same mains voltage as that supplied to the indicator tube.

and the delay in the ignition of the main discharge.

Some of the oscillograms recorded are drawn in *fig. 12*. The curves in fig. 12*a* refer to the main-discharge current. It can be seen that they are all of the same form, indicating a uniform build-up time, but that they are somewhat displaced with respect to each other. This spread amounts to only a few microseconds. The extremes lie about 10 μsec apart. The curves in fig. 12*b* represent the sum of certain fractions of the currents of both discharges, obtained by suitable choice of the resistances in the circuit of fig. 11; the ratio of the fractions selected was thus not the same in both recordings. From this fact and from the appearance of the curves we may conclude that the first peak to occur is due to the auxiliary discharge, and the second to the main discharge. The ignition of the main discharge is seen to begin less than 5 μsec after the first peak. This "take-over time" and also the build-up time (cf. fig. 12*a*) are found to be virtually constant. The spread in the total delay time is therefore almost entirely due to the spread in the statistical delay.

From the result of the above experiments we may deduce that the effects involved here have no influence on the maximum permissible frequency of the supply voltage. The measured time intervals are roughly 100 times smaller than the deionization time.

Owing to the fact that the total delay shows a certain spread, this does, as we have seen, have some influence on the minimum required amplitude of the control signal. This is evident since the spread in the total delay also causes a spread in the breakdown voltage which is equal to the delay multiplied by the time derivative of the supply voltage at the value of the breakdown voltage (about 130 V). This time derivative is greater the greater the amplitude of the supply voltage, the frequency remaining constant, and also the higher the frequency is raised with the amplitude remaining constant. An idea of the magnitude of this effect is given by the following numerical example, using values encountered in practice. Taking a frequency of 50 c/s, an amplitude of 300 V and a difference in delay time of 10 μsec for two breakdowns, then the ignition voltages of these discharges differ in value by about 0.85 V; at an amplitude of 150 V they differ by about 0.35 V. Compared with a signal amplitude of 3 or 4 V, these amounts are not entirely negligible.

It may be inferred from the foregoing that the tube can only be fed with a square-wave voltage if the steepness of the square-wave edges is less than about 10^5 V/sec; otherwise, the minimum required control signal will be considerably increased.

In this connection it should be noted that the minimum control voltage is smaller the closer the

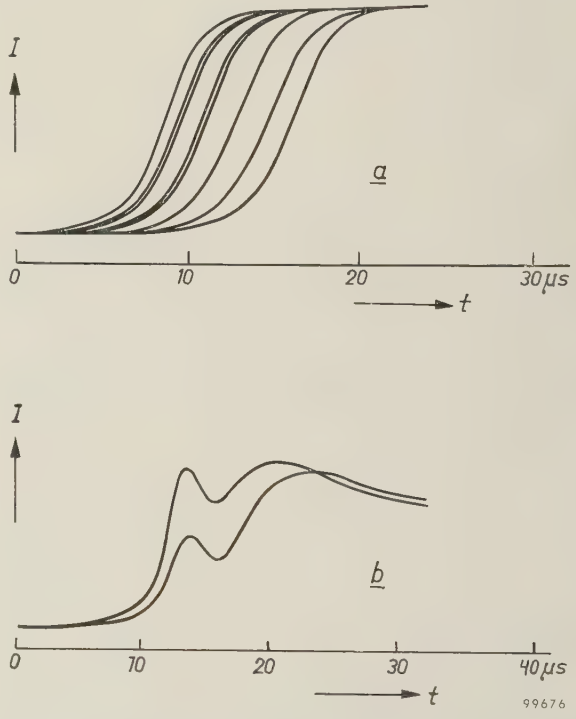

Fig. 12. *a*) Oscillograms of the main-discharge current. The curves are all of virtually the same form, indicating a constant build-up time, but there is a spread of some microseconds between the start of each curve (statistical delay). The outside curves lie less than 10 μsec apart.
b) Two oscillograms displaying the "summed" currents of auxiliary and main discharges. For both curves, the resistances in the circuit (fig. 11) are so chosen that the contribution of the auxiliary discharge current to the total signal is exaggerated with respect to that of the main-discharge current. In the one curve the ratio of the two contributions is different from the other curve. From the difference between the two it may be concluded that the first peak is due to the auxiliary discharge and the second to the main discharge. The main discharge is seen to ignite a few microseconds after the auxiliary current has reached its maximum.

electrode to which the discharge is to be transferred. In the light of what has been said in this section, this phenomenon is perfectly understandable. The electrons that initiate the avalanche in our tube originate, as a rule, from the discharge that took place during the preceding mains cycle. These electrons obviously diffuse faster and in greater numbers to nearby electrodes than to more distant ones. In regard to the discharge on these electrodes the statistical delay is therefore not only smaller but shows a smaller (absolute) spread, and hence gives a smaller spread in ignition potential.

It is due to this electron supply by diffusion that the statistical delay is as small as mentioned above. If the tube has been switched off for some time, so that the first electron must originate from another source, the delay may be appreciably greater. This does not, of course, prove troublesome in actual operation.

Visibility of the discharge

The visibility of a glow discharge depends on the nature of the gas and on the current density of the discharge. As already mentioned, the new indicator tube is filled chiefly with neon gas. From the viewpoint of light output neon is the best among the inert gases (other gases are chemically too reactive in gas discharges).

The current density is stepped up by choosing a fairly high gas pressure — the current density being roughly proportional to the square of the gas pressure — and also by producing an anomalous glow-discharge (cf. fig. 6).

Measurements have shown the brightness of the discharge to be about 1200 cd/m^2 (current density 10 mA/cm^2). This may be compared with the brightness of a 40 W fluorescent lamp, which is about 8000 cd/m^2. Partly because of its orange-red colour, the glow discharge is still clearly perceptible in normal daylight.

The anomalous discharge in the new tube is made possible by limiting the surface area of the cathodes; this also makes the indication easier to read. Without such limitation there would still be a glow discharge (in this case a normal one) near the trigger carrying the control signal, but it might take up quite an asymmetrical position in relation to that trigger.

Summarizing, it can be said that the new tube satisfactorily meets the existing need for a simple, easily readable decade indicator capable of being actuated by a low-energy signal of only a few volts. Tests have shown that the properties of the tube remain remarkably constant, both after intensive use and after long storage. The life of the tube, like that of other glow-discharge tubes, is expected to be very long.

———

Summary. For the read-out of transistor scaling circuits there is a need for indicator tubes (that do not themselves count) capable of being operated by low-energy signals of a few volts. The tube described has a flat annular cathode, the surface of which is divided into ten sectors, and a ring-shaped anode; the tube is filled with Ne + 0.1% Ar at a pressure of about 15 cm Hg. A gas discharge (anomalous glow discharge) is initiated at the desired place in the tube by means of one of ten auxiliary electrodes (triggers). The control signals supplied by the transistor circuit need only make the potential of the relevant trigger differ by 5 V from that of the (earthed) anode. The current of the auxiliary discharge required to initiate the main discharge is a mere 50 μA. The displacement of the main discharge to any desired position, corresponding to a given count, is made possible by the periodic extinction of the discharge. To this end the tube is fed with an unsmoothed, rectified alternating voltage, obtainable e.g. from the mains.

EXPERIMENTS WITH RADIOACTIVE PREPARATIONS OF THE ACARICIDE "TEDION V 18" *)

by J. HALBERSTADT **).

632.951.001.4:539.16

Under the proprietory name "Tedion V 18", Philips-Duphar are marketing preparations which destroy the eggs and larvae of mites, including the dreaded spider mite or "red spider" [1]). Trees treated with "Tedion" retain a residue which continues to exert its acaricidal action over a long period [2]). Tedion is not injurious to the tree, and is only very mildly toxic to warm-blooded animals.

In research on pesticides (the collective name for insecticides, acaricides, etc.) it is important to have quantitative data on the assimilation, transport and breakdown of these substances in the plant. In regard to their toxicity to warm-blooded animals, information is needed concerning the part the substances play in the metabolism of the animal (i.e. to what extent they are stored in the tissues and excreted from the body). An exact method of obtaining such data is provided by the use of radioactive tracers. The pesticide is "labelled" by partial replacement of one of its constituent elements by a radioactive isotope; the activity of the plant or animal treated with the pesticide is then measured to trace the distribution or location fo the tracer element.

This method has been adopted in the case of Tedion. The active ingredient of Tedion is 2,4,5,4′-tetrachlorodiphenyl sulphone:

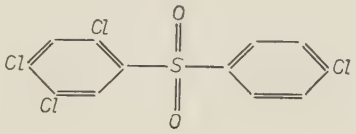

By a process briefly described elsewhere [3]) this substance is labelled with the β-active isotope of sulphur, ^{35}S. The half-life of the isotope is 87 days. Preparations with this compound have been used in field experiments on apple trees and in experiments on the metabolism of rats. A brief account of both types of experiment is given below.

Experiments on apple trees

The experiments on apple trees were done with Tedion in two formulations, viz. as a *wettable powder* and as *miscible oil* (emulsifiable concentrate) [4]). Two grams of the powder (containing 20% by weight of Tedion) were suspended in two litres of water, and 5 millilitres of miscible oil (Tedion content 8%) were emulsified in two litres of water. In the grounds of the Boekesteyn Agrobiological Laboratory [5]) two apple trees of the "Golden Delicious" variety were carefully sprayed with each of these liquids. This was done at the beginning of July 1957, when the weather conditions were favourable. The specific radioactivity of the Tedion preparation was then 6.1 millicuries per gram.

The objects of the experiments about to be described were to determine the amount of Tedion that settled *on* the leaves, the amount that penetrated *into* the leaves, and the manner in which both amounts changed in the course of time.

As soon as the leaves had dried, two samples were taken of 20 leaves each. Like all subsequent samples, these were immediately subjected to the following treatment. First, the leaves were cut lengthwise in two. The 20 left halves were at once dried out for eight hours at 40 °C and then reduced to powder, after which the total radioactivity of this powder was measured. The 20 right halves were washed in nitromethane to remove the radioactive Tedion on the surface (nitromethane is the only known solvent for Tedion that does not attack the leaves). These half leaves were thereupon dried and pulverized like the others, and the radioactivity of the internal Tedion was then determined.

The radioactivity measurements were done on "infinitely thick" powder preparations in an experimental arrangement employing a Philips Geiger-Müller counter type 18 506, with end window, and a Philips counting unit, type PW 4035. The variation in the results of the measurements was about 3%.

To ascertain from the radioactivity the amount of Tedion taken up in the leaf samples, a comparison

*) Trade mark.

**) Now with the International Atomic Energy Agency at Vienna, formerly with N.V. Philips-Duphar, Weesp (The Netherlands).

[1]) J. Meltzer, Research on the control of animal pests, Philips tech. Rev. **17**, 146-152, 1955/56, in particular page 152.

[2]) J. Meltzer and F. C. Dietvorst, Action of Tedion on eggs and ovaries of spider mites, T. Planteziekten **64**, 104-110, 1958.

[3]) J. Halberstadt, Some experiments with radioactive preparations of 2,4,5,4′-tetrachlorodiphenyl sulphone, a new acaricide, Meded. Landbouwhogeschool en Opzoekingsstations van de Staat te Gent **23**, 788-794, 1958.

[4]) W. Duyfjes, The formulation of pesticides, Philips tech. Rev. **19**, 165-176, 1957/58.

[5]) Philips tech. Rev. **16**, 353, 1954/55.

sample was prepared. For this purpose 2.54 g of dry leaf powder, obtained from ten leaves that had not been sprayed, was mixed with a solution of 0.254 mg of radioactive Tedion, and again dried.

A comparison of the activities does not, however, yield directly the amount of Tedion but rather the amount of sulphur atoms introduced by the Tedion into the leaves. These belong only partly to chemically unaffected molecules of Tedion; the remainder of the sulphur has been incorporated in the plant in the form of glucosides or proteins, or is contained in the break-down products of the Tedion.

In order to discover what proportion of the sulphur was still present in free molecules of Tedion, the method of isotopic dilution analysis was used. A weighed amount of non-radioactive Tedion is added to the dried leaf material, and the Tedion is then extracted from the mixture with the aid of a suitable solvent. In this way the radioactive Tedion already present in the leaf powder is obtained in a solution together with the added non-radioactive Tedion. After concentration of the solution the Tedion largely crystallizes out. This preparation is purified by recrystallizing it until the melting point and the specific activity are constant. Let the latter be a and let that of the Tedion sprayed on the tree be a. If x milligrams is the original amount of radioactive Tedion present in the leaf powder, and g milligrams is the added amount of non-radioactive Tedion, then

$$a\,x = a'(g + x).$$

Since x is very small compared with g, we can write

$$x = \frac{a'}{a}\,g.$$

In *fig. 1* the results are given in micrograms of Tedion-sulphur per leaf as a function of the time between the spraying of the tree and the taking of the leaf sample. Fig. 1*a* relates to the wettable powder, and fig. 1*b* to the miscible oil. It is seen that with both formulations the "external" sulphur, i.e. *on* the plant (△---△), drops in one to two days to half its initial value. (The fall-off in inherent activity of the ^{35}S — half-life 87 days — can be neglected here.) There was no rainfall after spraying until after the second leaf sample had been taken, so that this result cannot be attributed to rain. After about four days 20% of the powder preparation remains on the leaf and 40% of the miscible-oil preparation. Thereafter the amount of external sulphur diminishes slowly until, in about three months, there is virtually none left; the total activity is then equal to the

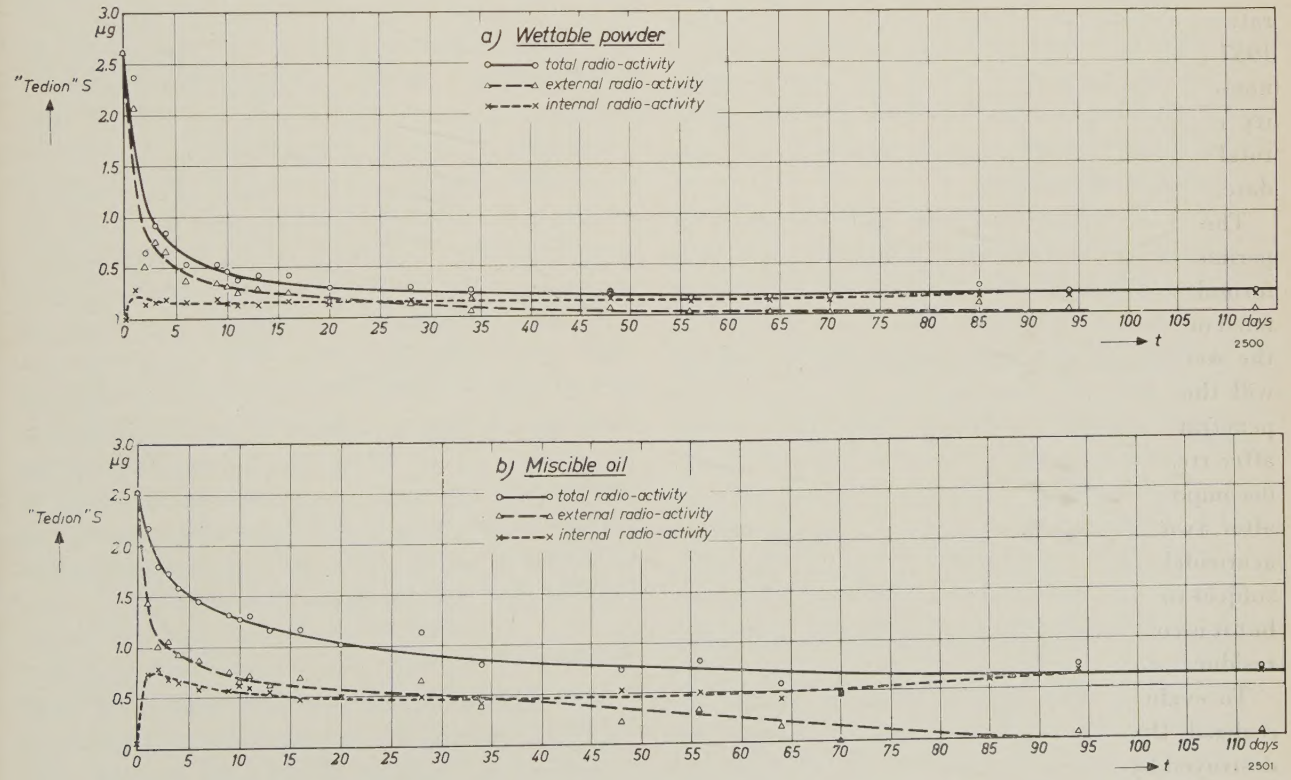

Fig. 1. Amount of Tedion-sulphur per leaf, as a function of the number of days following the spraying of apple trees with a preparation of *a*) wettable powder, and *b*) miscible oil.

"internal" activity, i.e. the activity of the sulphur inside the leaves.

The amount of this internal sulphur (× - - - ×) in fig. 1*a* and *b*) shows initially a rapid increase and in both formulations it reaches a maximum in about one day. This maximum is roughly equivalent to 8% of the activity of the total sprayed Tedion in the case of the wettable powder, and 30% in the case of the miscible oil. The leaves treated with the miscible-oil preparation thus take up almost four times as much Tedion as the leaves sprayed with the powder preparation (this proportion is also subject, of course, to other factors, such as the size of the particles on the leaf, the nature of the contact between the particles and leaf, etc.).

Beyond the maximum, the internal sulphur slowly diminishes to a value that remains constant for about a month; for the miscible-oil preparation this value is approximately three times higher than for the wettable powder. After about two months the internal sulphur showed a slight increase in both cases. This may be due to the fact that, at the end of the summer season, all life processes in the leaves — including those that break down the Tedion — begin to slow down, although the take-up of external residues presumably continues undiminished.

The method of isotopic dilution analysis, applied to the leaf samples treated with miscible-oil preparation, yielded the following results. In November 1957 (141 days after spraying) 79.2 micrograms of non-decomposed Tedion were found, with an activity of 0.157 microcuries ^{35}S. This is 17.5% of the total activity of the leaf sample, which, on the same date, was 0.9 microcuries.

The conclusions drawn from the leaf-sample experiments were the following. From the miscible-oil formulation three to four times as much Tedion is fixed on the leaf and taken-up inside the leaf as from the wettable-powder formulation. The miscible oil will thus be more economical in use. The Tedion penetrates quickly into the leaf. More than a month after treatment there is still a fair amount of non-decomposed Tedion left on and in the leaf, and even after two months enough remains to exercise an acaricidal action. The Tedion taken up in the leaf is subject to conversion and transport inside the plant, but it is continuously supplemented from the surface residue.

To evaluate these findings correctly, it must be realized that the eggs and larvae of mites are destroyed by contact with Tedion, and that the eggs laid by a fully-grown mite that has fed on the leaf sap will not hatch out if the Tedion content in the sap is sufficiently high. Effective mite control therefore requires the presence of Tedion *on* as well as *in* the leaf. Tedion is found to meet both requirements most satisfactorily.

Generally speaking, it is desirable that a pesticide applied to cultivated plants should be broken down by the plant at such a rate that little or none is left when the time comes for the plant or its fruits to be consumed by man or domestic animal. Tedion, which is in any case virtually innocuous to mammals, actually undergoes such a slow break-down.

We shall now touch on the experiments relating to the *fruits* of the sprayed trees. Apples, picked about 6½ weeks after spraying, were first washed in warm nitromethane to dissolve the surface Tedion. They were then peeled, after which the peelings and the fruits were separately reduced to pulp and the pulp masses extracted with a chloroform solvent. Only unchanged Tedion is extracted in this way. The two chloroform extracts were evaporated to dryness and the residues dissolved in nitromethane. Measurements were then made of the radioactivity of the three nitromethane solutions (but not of the extracted pulp). The results are given in *Table I*.

Table I. Measured radioactivity of apples 6½ weeks after spraying the trees with radioactive Tedion in different formulations.

Tedion formulation	Part of apples	Per five apples:	
		Microcuries of ^{35}S	Calculated Tedion content, μg
Miscible oil	On peel	0.127	30
	In peel	0.096	23
	In fruit (extract)	0.077	18
			71
Wettable powder	On peel	0.035	9
	In peel	0.013	3
	In fruit (extract)	0.033	8
			20

In all, five apples took up 71 μg of Tedion from the miscible oil and 20 μg from the wettable powder (i.e. roughly the same proportions as found in the leaves). Both amounts are too small to exercise an acaricidal action and *a fortiori* are insignificant as regards their possible toxicity to man.

Experiments on rats

The experiments on rats were done with a preparation consisting of a suspension of radioactive Tedion in an emulsion of salad oil in water. The specific radioactivity of the Tedion amounted to a few millicuries per gram. In the first experiments

the rats were given a total dose of 100, 50 or 10 milligrams of Tedion per kilogram of bodily weight, either at once or spread over several days. The preparation was introduced directly into the stomach through a catheter.

As a preliminary experiment a number of rats received daily one tenth of the total dose (100 mg) for ten days. Some of these rats were then killed, and some of their organs and tissues were examined for radioactivity by various chemical extraction techniques. The rats not killed were left under normal conditions in their cages and the activity of their faeces and urine was tested.

In a subsequent experiment a total amount of 100, 50 or 10 mg of radioactive Tedion per kg bodily weight was administered to rats in a single dose. After 48 hours these rats were killed and their organs and tissues, as well as their collective faeces and urine, were tested for radioactivity. Details of the methods employed will be described elsewhere.

The preliminary experiment showed that many tissues had become radioactive, especially fatty tissues, the tissue of the gastro-intestinal tract, muscles and liver. The hair, too, showed slight radioactivity, indicating that part of the Tedion had been broken down into simpler sulphur compounds from which, by biosynthesis, sulphur-amino acids had formed that are found in hair. By far the greater part of the Tedion, however, was found to have left the body of the rats: 71% with the faeces, 4% with the urine, and 7% was still present in the contents of the intestinal tract. It may therefore be assumed that 82% of the administered dose is excreted and that a mere 18% is taken up in various parts of the body. After the dosage was stopped the radioactivity in the living rats dropped rapidly to a negligible value. *Table II* gives a survey of the distribution found in a rat which had received 100 mg per kg in a single dose. The sum of the amounts of sulphur determined by radioactivity measurements (1236 μg) agrees remarkably well with the administered dose (1221 μg), a fact which strengthens our confidence in the method employed.

The same experiment was done on two other rats with a dose of 50 mg Tedion per kg, and on another two with 10 mg per kg. The relative distribution over the various constituents of the body differed very little from that shown in Table II.

Isotopic dilution analysis was used to ascertain what percentage of the measured radioactivity of the various body constituents was due to non-decomposed Tedion. Without going into details, we may mention the general conclusion that, of the administered 100 mg of Tedion per kg bodily weight, 40 to 45% was found unchanged after 48 hours, mainly in the faeces. Thus, 55 to 60% is broken down in one way or another, presumably to a large extent by the action of the bile.

Table II. Distribution of Tedion-sulphur in the body of a rat, 48 hours after receiving a dose of 13.6 mg of Tedion (i.e. 1221 μg of sulphur). The rat weighed 136 g.

Constituents analysed		Tedion-sulphur in μg
Faeces		878.8
Urine		51.3
Skin and hair	acetone extract (cutaneous fat)	87.8
	residue (mainly hair)	5.2
Gastro-intestinal tract tissue		84.4
Muscles		16.9
Fat		78.1
Blood (major part)		0.10
Brains		0.16
Heart		0.10
Kidneys		0.39
Liver		4.14
Lungs		0.43
Spleen		0.06
Carcass (unspecified remainder of body, largely bone, gristle and sinew)		24.3
Cage swill		4.23
	Total	1236.41 ± 20

The experiments described provide no answer to such questions as: Where in the plant or the body of the animal is the Tedion decomposed? and: What are the decomposition products? Investigations along these lines are in progress. In conclusion it may be remarked that the foregoing gives further evidence, if any were needed, of the great value of radioactive-tracer techniques to biological research.

Summary. Radioactive-tracer techniques are applied to investigations into the behaviour in plants and animals of "Tedion V 18" (an acaricide for the control of spider mites). The sulphur in the active ingredient of Tedion, which is 2,4,5,4′-tetrachlorodiphenyl sulphone, is partly replaced by the radioactive isotope ^{35}S. Apple trees were sprayed with preparations of this radioactive Tedion in two formulations: as a wettable powder and as a miscible oil. Radioactivity measurements showed that an active residue remains *on* the leaf for a long period, whilst the Tedion taken up *in* the leaf is subject to conversion and transport within the plant, being continuously supplemented from the surface residue. The miscible oil proves to be more economical in use than the wettable powder. Administered to rats (max. dose 100 mg per kg bodily weight), about 40 to 45% of the Tedion is found unchanged after 48 hours, mainly in the faeces; the remainder is broken down.

ABSTRACTS OF RECENT SCIENTIFIC PUBLICATIONS BY THE STAFF OF N.V. PHILIPS' GLOEILAMPENFABRIEKEN

Reprints of these papers not marked with an asterisk * can be obtained free of charge upon application to Philips Electrical Ltd., Century House, Shaftesbury Avenue, London W.C. 2, where a limited number of reprints are available for distribution.

2696: H. C. Hamaker: Attributenkeuring in theorie en praktijk (Statistica neerl. **13**, 37-58, 1959, No. 1). (Theory and practice of sampling by attributes; in Dutch.)

This paper brings a survey of present-day theory and practice of sampling by attributes. In section 2 the main points in the theory of OC-curves are recapitulated. Section 3 lists the various features which people have attempted to incorporate in sampling tables, and the various factors which influence our choice of a sampling plan. Subsequent sections discuss economic theories, the importance of the distribution of the percentage of defective items over the inspection lots, the relation between sample size and lot size, and some of the existing sampling tables. In a final section the possibilities for further improvements in existing sampling practices is considered. One conclusion is that in many situations a constant sample size regardless of lot size would have very definite advantages.

2697: A. Claassen and L. Bastings: The gravimetric determination of nickel with dimethylglyoxime in the presence of copper (Z. anal. Chemie **165**, 354-360, 1959, No. 5).

A detailed investigation has been made of the gravimetric determination of nickel with dimethylglyoxime in the presence of copper. Copper interference is eliminated by precipitation in a solution containing tartrate and thiosulphate at a *p*H of 5.5-6.5. The solubility of the nickel dimethylglyoxime complex has been determined as a function of temperature, *p*H and alcohol concentration.

R 385: K. Teer: Investigations into redundancy and possible bandwidth compression in television transmission (Philips Res. Repts. **14**, 501-556, 1959, No. 6).

In this thesis (Delft, Sept. 1959) the possibility of bandwidth compression in television transmission is considered. Three different aspects of redundancy present in normal television transmission are considered: (1) the statistical aspect, which is concerned with probability distributions of brightness, (2) the physiological aspect, which is concerned with the properties of the eye (resolving power, persistence of vision, differential sensitivity and colour perception), (3) the psychological aspect, which is related to levels of consciousness. After this analysis of redundancy, transmission systems of narrow bandwidth are described which have been investigated by the author. In all these systems bandwidth compression is effected by a decrease in the number of frames per second, viz., by decreasing the field frequency or the information per field. For practical realization of the former method a suitable memory device is needed. Considerations are restricted to the memory device, in particular to a vidicon-type camera tube, which can be used as a fairly simple device of this kind. A decrease of the information per field can be realized by use of dot-interlace and subcarrier techniques, which are examined in detail. Finally, the use of these principles in colour television is considered, mainly with the N.T.S.C. system and a two-subcarrier system.

R 386: F. A. Kröger, F. H. Stieltjes and H. J. Vink: Thermodynamics and formulation of reactions involving imperfections in solids (Philips Res. Repts. **14**, 557-601, 1959, No. 6).

Two types of formulation of reactions involving imperfections in solids are analysed and compared with each other. As a result it appears that, in Schottky's system, the amount-of-substance variables mostly refer to relative building units. Therefore true thermodynamic potentials can be assigned to them and they also can appear as components in the phase rule. In an alternative system the amount-of-substance variables do not refer to building units, but to structure elements and to associates between them. To those no true thermodynamic potential can be assigned. However, by introducing virtual thermodynamic potentials for them, all problems can be dealt with, often in a much more convenient way than with the other type of formulation. Also, appearing as quasi-components in the phase rule, they greatly facilitate its handling. This is illustrated by treating with the aid of the structure-element system various cases of disorder. For the description of those properties of a crystal which are not related to the thermodynamics of reactions, the use of structure elements is also of advantage.